

Washington University in St. Louis
Washington University Open Scholarship

All Theses and Dissertations (ETDs)

1-1-2010

Antimicrobial Effect of Transition Metal Oxide Nanoparticles

Zhipeng Wang

Washington University in St. Louis

Follow this and additional works at: <https://openscholarship.wustl.edu/etd>

Recommended Citation

Wang, Zhipeng, "Antimicrobial Effect of Transition Metal Oxide Nanoparticles" (2010). *All Theses and Dissertations (ETDs)*. 517.
<https://openscholarship.wustl.edu/etd/517>

This Thesis is brought to you for free and open access by Washington University Open Scholarship. It has been accepted for inclusion in All Theses and Dissertations (ETDs) by an authorized administrator of Washington University Open Scholarship. For more information, please contact digital@wumail.wustl.edu.

WASHINGTON UNIVERSITY IN ST. LOUIS

School of Engineering and Applied Science

Department of Energy, Environmental and Chemical Engineering

Thesis Examination Committee:

Dr. Yinjie Tang, Chair

Dr. Da-Ren Chen

Dr. Young-Shin Jun

ANTI-MICROBIAL EFFECTS OF TRANSITION METAL OXIDE
NANOPARTICLES (NPs)

By

Zhipeng Wang

A Thesis presented to the School of Engineering
of Washington University in partial fulfillment of the requirements of the
degree of

MASTER OF SCIENCE

May 2010

Saint Louis, Missouri

ABSTRACT

The eco-toxicity of six types of transition metal oxide nanoparticles (NPs) (TiO_2 , NiO, ZnO, CuO, Co_3O_4 and Fe_2O_3) was studied extensively both in aqueous culture medium and under aerosol exposure (spraying these particles directly on cell surface). In the aqueous medium, only NiO NPs showed strong inhibition (>30%) to cell growth when concentration was over 2mg/L. In contrast to aqueous exposure where the particles and bacteria had limited interactions, aerosol exposure of three metal oxide NPs to *E.coli* enhanced NPs' toxicity to cells and dramatically reduced cellular viability: electro spraying of NiO, CuO and ZnO NPs (20nm, 20 μg , in 10mins) reduced the total number of living *E.coli* compared to the control experiments by more than 88%, 77% and 71% respectively. Spraying larger ZnO NPs (480nm, 20 μg , in 10min) caused much less lethality to *E.coli* cells, which indicated the NPs' toxicity was associated with nano-size effect. On the other hand, electro spraying of other two types of metal oxide NPs (TiO_2 and Co_3O_4) decreased the lethality to cells (to below 20%). The reason was due to their extremely low solubility in aqueous medium. Fe_2O_3 NPs showed no antibacterial activities under both aqueous exposure mode and aerosol exposure mode. Furthermore, we extended eco-toxicity study to different bacterial species using ZnO NPs. Five types of microorganisms have been investigated: pathogenic bacteria (non-virulent species *Mycobacterium smegmatis*), metal reducing bacteria (*Shewanella oneidensis* MR-1), blue-green algae (*Cyanothece* 51142), yeast (*Saccharomyces Cerevisiae*), and enterobacterium (*Escherichia coli*). *Shewanella oneidensis* MR-1 and *Escherichia coli* could tolerate the ZnO NPs' stress in the aquatic mode, while *M.smegmatis* and *Cyanothece* 51142 could be inhibited seriously in a dose response manner in the aquatic mode. Further studies showed that the antimicrobial activities of aerosolized metal oxide NPs were mainly determined by three key factors: 1) the solubility of particles; 2) the toxicity of the metal ions; 3) the mode of exposure. The above observations provided the guidelines for potential application of electro sprayed NPs to disinfect airborne pathogens.

Contents

ABSTRACT.....	ii
List of Tables	v
List of Figures.....	vi
Chapter 1	1
1.1 Introduction.....	1
1.2 Eco-toxicity of NPs in the aqueous culture.....	2
1.3 Exposure of NPs to biological systems.....	6
1.4 Research objectives.....	8
1.4.1. Investigate the nano-related toxicity other than ionic stress in both aerosol exposure and aquatic modes.....	8
1.4.2. Systematically test ZnO NPs' eco-toxicity to different microorganisms.....	9
1.5 Outline of the thesis.....	9
Chapter 2.....	11
2.1 Growth of cells with NPs in aqueous mode	11
2.2 Aerosol exposure of NPs to E.coli	12
2.3 Analytical measurements	15
2.3.1 DNA release	15
2.3.2 GFP expression.....	15
2.3.3 EPS production.....	16
2.3.4 Measurement of soluble ions.....	16
2.4 SEM and TEM protocols.....	17
Chapter 3.....	19
3.1 Effect of metal oxide NPs on microbial growth.....	19
3.2 Effect of aerosolized metal oxide NPs on microbial survival.....	21
3.3 Mechanisms of metal oxide NPs' antibacterial activities	24

3.4 Biological responses and dissolution of transition metal oxide NPs	25
Chapter 4.....	28
4.1 Effect of ZnO NPs on microbial growth in aquatic exposure mode	28
4.2 Aerosol exposure of ZnO NPs to cells using electrospray.....	33
Chapter 5.....	39
5.1 Conclusion.....	39
5.2 Acknowledgements	40
Appendix.....	41
Project A.....	41
Project B.....	46
References.....	49
Vita.....	55

List of Tables

Table 3-1. Responses of <i>E. coli</i> to NPs and metal ions in the aqueous phase.....	20
Table 3-2. Release of metal ions (mg/L) from metal oxide NPs (20 mg/L) in the aqueous phase	20
Table 3-3. Percentage (%) of <i>E.coli</i> viability reduced after exposure to aerosolized metal oxide NPs (comparing to exposure to particle free buffer solution)*	22
Table 3-4: Released DNA in the aqueous phase (20 mg/L) and after electrospraying and solubility in the aqueous phase (20 mg/L).....	26
Table 4-1. Inhibition to microbial biomass production (initial OD ₆₀₀ =0.1) and GFP production of <i>E. coli</i> in the presece of ZnO NPs (n=3).(Wu B et.al.2010b).....	29
Table 4-2. EPS production under the stress of ZnO NPs (20 nm, 20 mg/L) during the exponential growth phase (n=3). (Wu B et.al.2010b).....	32

List of Figures

Figure 1-1. Responses of <i>M. smegmatis</i> to NPs (0.02 g/L) (n=2); (○) Control; (∇) 1.8%-Cu-doped TiO ₂ NPs; (□) 0.6%-Cu-doped TiO ₂ NPs; (◇) TiO ₂ NPs. (Wu B et.al. 2009)	4
Figure 1-2. SEM and TEM images of cells with 1.8%-Cu-doped TiO ₂ NPs; (a) SEM of <i>M. smegmatis</i> ; (b) TEM of <i>M. smegmatis</i> . (Wu B et.al. 2010a).....	5
Figure 1-3 Electro spray devices.....	8
Figure 2-1 Electro spray experimental set-up	13
Figure 3-1. SEM images of <i>E.coli</i> with NPs	21
Figure 3-2. The growth recovery of <i>E.coli</i> in a M9 minimum medium after electro spraying transition metal oxide NPs (20µg) (n=3); (□) After electro spraying buffer; (Δ) After electro spraying TiO ₂ NPs; (◇) After electro spraying CuO NPs; (○) After electro spraying NiO NPs.....	23
Figure 4-1. Sensitivity of <i>M. Smegmatis</i> (initial OD ₆₀₀ =0.01) to the dose of ZnO NPs (20 nm). (●) control; (■) 0.2 mg/L; (□) 0.5 mg/L; (◆) 2 mg/L; (◇) 20 mg/L. Error bars were the standard deviations (σ) of the replicate analyses.(Wu B et.al.2010b).....	30
Figure 4-2. SEM and TEM images of ZnO NPs (20 nm) and ZnO NPs with bacterial cells. (A) ZnO NPs in the aquatic medium (pH 7.0); (B) ZnO NPs after electro spray; (C) ZnO NPs (20 mg/L) with bacteria (<i>M. smegmatis</i>) in the aquatic medium; (D) Aerosol exposure of ZnO NPs on bacterial surface (<i>E. coli</i>). (Wu B et.al. 2010b).....	34
Figure 4-3. Investigation of toxicity after <i>E. coli</i> was electro sprayed with NPs (n=3) (1) initial viable <i>E. coli</i> deposited on the membrane; (2) viable <i>E. coli</i> after electro spraying water (without NPs); (3) viable <i>E. coli</i> after electro spraying 30 mg/L ZnCl ₂ solution (total 3.2 µg Zn ²⁺); (4) viable <i>E. coli</i> after electro spraying buffer (as the control experiment); (5) viable <i>E. coli</i> after electro spraying buffer with ZnO NPs (20 nm, 4 µg), P-value=0.002; (6) viable <i>E. coli</i> after electro spraying buffer with ZnO NPs (20 nm, 20 µg), P-value=0.01; (7) viable <i>E. coli</i> after electro spraying buffer with ZnO NPs (480 nm, 4 µg), P-value=0.01; (8) viable <i>E. coli</i> after electro spraying buffer with TiO ₂ NPs (20 nm, 4 µg), P-value=0.19. (Wu B et.al. 2010b).....	35
Figure 4-4. Growth curves of <i>E. coli</i> in the aquatic medium (n=3) (□) <i>E. coli</i> in the aquatic medium without ZnO NPs; (◆) <i>E. coli</i> in the aquatic medium with ZnO NPs (100 mg/L, 20 nm); (■) <i>E. coli</i> cells were transferred from the membrane to liquid medium after electro spraying ZnO NPs (4 µg, 20 nm). (Wu B et.al. 2010b)	37
Figure A-1. SEM and TEM images of the Ag nanocubes (a) and the Au-Ag nanocages (b-d) used in this study. The scale bars are 500 nm and 100 nm for SEM and TEM (inset) images respectively. (e)	

Absorbance spectra of the nanocubes and nanocages. The nanocages were prepared from the nanocubes in (a) via the galvanic replacement reaction and their LSPR was tuned to 525 nm (b), 620 nm (c), and 790 nm (d). The vertical lines in (e) correspond to the wavelengths of the excitation sources used in this experiment. (M.Rycenga and Zhipeng Wang et.al. 2009) 43

Figure A-2. (a) The SERS spectrum of aqueous 1-DDT nanocubes at different solution temperatures with 514 nm excitation. The temperature of the solution was controlled with a temperature control stage. The spectrum contains the gauche (G) 1080 cm^{-1} and trans (T) 1125 cm^{-1} carbon-carbon stretch of the 1-DDT SAM with the scale bar corresponding to 10.8 $\text{adu mW}^{-1} \text{s}^{-1}$. The relationship between temperature and peak intensities of the T and G bands are shown in (b), where an increase in the solution temperature causes the T band to attenuate and the G band to increase. (M.Rycenga and Zhipeng Wang et.al. 2009)..... 44

Figure A-3. Results of molecular dynamic simulations of 1-DDT SAMs (a) Optimized alkane chain conformation of a 1-DDT SAM on a Au surface at three different temperatures. The cartoons are looking down the carbon chain toward the sulfur group where grey is carbon, white is hydrogen and yellow is sulfur. When the temperature was increased, the torsion of the alkyl chains increased and there is a higher population of end-gauche and gauche conformations as evidenced by the increasing non-planar character of the alkane thiol molecule. (b) A plot of the Trans/gauche ratio of the 1-DDT SAM from experimental (square markers) and simulation (triangle markers) data. Table 1 shows the derived temperatures of the 1-DDT SAMs on the nanocages from the fits in (b). (M.Rycenga and Zhipeng Wang et.al. 2009)..... 45

Figure B-1 Experimental set-up for CO₂ shock on *Shewanella oneidensis* MR-1 in liquid medium (Schematic Picture of the reactor)..... 47

Figure B-2. The AFM (Atomic Force Microscopy) images for *Shewanella oneidensis* MR-1 before and after the CO₂ shock (5min). (Wu B et.al. submitted) 48

Chapter 1

1.1 Introduction

Transition Metal Oxide NPs have wide applications in industrial materials, medical research, environmental remediation, and energy generation (Adam et.al. 2006; Kwak et.al.2001). Recently, the eco-toxicity of transition metal oxide nanoparticles (NPs) from their unique behaviors in natural environments has attracted great attention (Franklin et.al. 2007; Limbach et.al. 2007; Aruoja et.al. 2009).

The eco-toxicity for nanomaterials is not a new concept. For example, carbon-based nanomaterials (CBNs) have been reported to cause significant cellular damage, which has contributed to their physical and chemical stresses on biological systems, or to light-triggered free radicals (Chen and Elimelech 2008; Kang et.al. 2008a; Kang et.al. 2009; Mauter and Elimelech 2008; Oberdoster et.al. 2005; Saleh et.al. 2008; Tang et.al. 2007). Furthermore, transition metal oxide NPs may cause even higher environmental concerns because of their unique dissolution properties, electronic charges, small size and large surface-to-mass ratio (Franklin et.al. 2007; Navarro et.al. 2008). The electronic structures of transition metal oxides have attracted much attention by chemists and physicists (Park et.al. 2001; Klosek et.al. 2000). Some transition metal oxides are semiconductors, which can play as photo-catalysts for degradation of organic and inorganic pollutants (Wei et.al. 1994; Klosek et.al. 2000). Similarly, they can be used to kill the bacteria with their photocatalytic properties (Wei et.al. 1994; Kim et.al. 2003). Taking TiO_2 as an example, when TiO_2 NPs are irradiated by UV-light (wavelength about 380nm), the electron-hole pairs will form, which can

trigger a series of redox reactions in biological systems. The electronic structures for semiconductors, in physical perspective, are composed of valence band, conduction band and band gap. Under the UV-light irradiation, the electrons from valence band are excited to the conduction band, which cause the formation of electron-hole pairs. The holes can capture the biological species and oxidize them, while the electrons can trigger reduction reactions. These physical properties have wide applications in industry as well as environmental engineering field. Through last decades, many researchers had focused on the study of eco-toxicity of transition metal oxide NPs with their unique photocatalytic behaviors (Edward et.al.2002; O.Seven et.al.2004; Hu et.al. 2006). As for the fast development of nanotechnology, this kind of research will continue to deepen our understandings of metal nanoparticles' biological functions and to provide potential new applications of these nanoparticles.

1.2 Eco-toxicity of NPs in the aqueous culture

Until recently, most studies have focused on the aquatic environment when testing the eco-toxicity of transition metal oxide NPs (Aruoja et al. 2009; Auffan et al. 2009; Brayner 2008; Franklin et al. 2007; Handy et al. 2008; Hu XK et al. 2009). The mechanism of eco-toxicity for transition metal oxide NPs in aquatic environment is relatively obscure. Most of the researchers agree that the eco-toxicity of transition metal oxide NPs in aquatic system mainly attributes to the toxicity of dissolved species. In other words, the metal ionic species play the key role in toxicity to biological systems in aquatic environment.

Compared to the toxicity of metal ionic species, the nano-associated toxicity (mechanical stress, physical damage, toxic compounds penetration etc) is still controversial. The reason is that the NPs tend to aggregate in aquatic medium, which can form relatively large agglomerates and reduce their nano-associated toxicity (Wu et.al. 2010a; Wu et.al.2010). The aggregation is driven by thermodynamic process to achieve the minimum surface energy. Therefore, NPs' toxicity is mainly controlled by its solubility in aqueous medium. The similar conclusion has been discussed by a recent paper published by our group (Wu B et.al. 2010a). The study focuses on the antimicrobial effects of TiO₂ NPs and Cu-doped TiO₂ NPs in aqueous culture medium with *Mycobacterium smegmatis* and *Shewanella oneidensis* MR-1. The key observations are: TiO₂ particles (<100mg/L) do not apparently inhibit the growth of the two species in aqueous culture; Cu-doped TiO₂ NPs (20mg/L) significantly reduce *M. smegmatis* growth rates by three folds (Fig 1-1). The Cu-doped TiO₂ NPs can release Cu²⁺ in aqueous solution so these kind of NPs cause toxicity to *M. smegmatis* (but not metal reducing bacterium *Shewanella*).

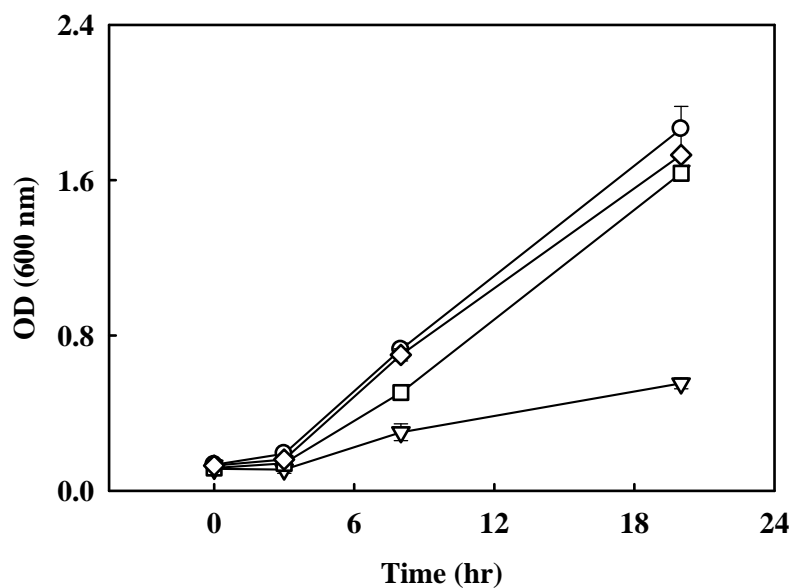


Figure 1-1. Responses of *M. smegmatis* to NPs (0.02 g/L) (n=2); (○) Control; (▽) 1.8%-Cu-doped TiO₂ NPs; (□) 0.6%-Cu-doped TiO₂ NPs; (◇) TiO₂ NPs. (Wu B et.al. 2009)

Fig 1-2 a) shows the SEM images of NPs with *M. smegmatis*. The NPs aggregate seriously so the particle size is actually near the micro-meter, the interaction between NPs and cells is not apparently observed. Fig 1-2 b) shows the TEM images of NPs with *M. smegmatis*, it is apparent that no NP penetrates into the cells, which indicates that the toxicity of NPs is mainly attributable to released ionic species.

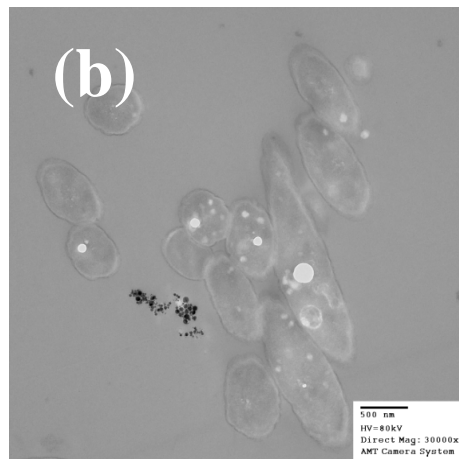
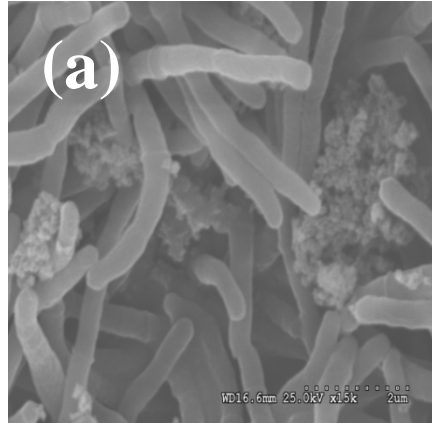


Figure 1-2. SEM and TEM images of cells with 1.8%-Cu-doped TiO₂ NPs; (a) SEM of *M. smegmatis*; (b) TEM of *M. smegmatis*. (Wu B et.al. 2010a)

Many studies have been done for investigating the eco-toxicity of transition metal oxide NPs in aquatic environment. One of the most interesting research topics is about the ZnO NPs. ZnO NPs are widely used as pigment, semiconductor, sunscreen, biosensor and food additive. Accompanying the various applications of ZnO NPs, studies on their toxicological level, fate, and behavior in the environment become critical to determine the potential risk of

their exposure. In aquatic environment, the ZnO NPs aggregate to micro-sized particles, which cannot interact with cells effectively. The toxicity of ZnO NPs in aquatic environment is mainly attributable to dissolved Zinc Species; some bacteria are very sensitive to ZnO NPs in aquatic environment. Recently, toxicity of ZnO NPs to a variety of microorganisms in aqueous environment has been reported (Adam et.al.2006; Brayner et.al.2008; Franklin et.al.2007; Hu et.al.2006). Several studies indicate that the release of Zn^{2+} from ZnO NPs in the aqueous environment determines the toxicity of NPs. Meanwhile, other studies have shown that metal NPs may be more toxic than their ionic forms or than their parent compounds (Navarro et.al.2008; Farre et.al.2009). Many experiments of investigating NPs' eco-toxicity have been conducted using *E. coli* or microalgae as model microorganisms. However, limited study has been done to compare cellular responses of different microorganisms to NPs.

1.3 Exposure of NPs to biological systems

The state of dispersion for ZnO NPs as well as other types of transition metal oxide NPs plays an important role for their toxicity to bacteria. A recent paper confirms that the state of dispersion alters NPs' eco-toxicity and reduces the influence of particle size, shape and surface charge on NPs' behavior (Handy et.al. 2008). Although quite a few methods have been commonly used for dispersion of NPs, such as addition of solvents (or dispersants), ultrasonication, and shaking (or stirring), they appear to have disadvantages in studying toxicity of NPs (Farre et.al. 2009). For example, the ultrasonication can change NPs' structure and

solvents tend to be toxic to the tested microorganisms. The synthesis of well dispersed NPs in aqueous solution has been reported (Sun et.al. 2002; Rycenga and Wang Z. et.al. 2009). But such NPs are difficult to be used for testing the ecotoxicity in aqueous solution; this is because the dispersants actually exist in the solution, which hinders the interaction between the NPs and bacteria.

To our knowledge, limited study has approached the uniform spray of metal oxide NPs to microorganisms (i.e., aerosol exposure mode), which results in the direct interaction between cells and NPs. One way to create the mono-dispersed nano-scale droplets is electrospray, which was originally invented by Cloupeau et.al. 1988. Electrospray, formally called “electro-hydrodynamic atomization,” is a technique used to convert a liquid solution or suspension into airborne droplets using both mechanical and electrostatic forces (Cloupeau et.al. 1989; Cloupeau et.al 1990; Cloupeau et.al.1994a; Cloupeau et.al.1994b) (shown in Fig 1-3). During the electrospraying process, the electric field enables the charged nano-sized particles to be separated and deposited on the ground surface. The method was further developed by Chen et.al. 1995. The developed method can create mono-dispersed aerosolized airborne droplets in the diameter range of 4nm to 1.8 μ m (Chen et.al. 1995). By controlling the droplet size and electrical charge of the droplets produced in the electrospray, ZnO NPs can be dispersed in nanoscale with minimal aggregation, thus offering a possibility to study the nano-effects of ZnO NPs on microbial species.

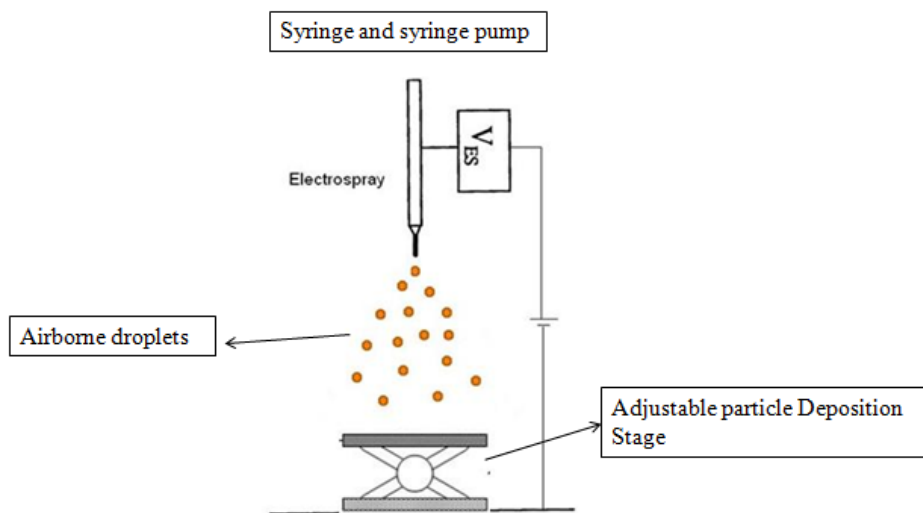


Figure 1-3 Electro spray devices

1.4 Research objectives

The research in this study has two objectives:

1.4.1. Investigate the nano-related toxicity other than ionic stress in both aerosol exposure and aquatic modes.

The airborne NPs' anti-microbial activities are very important for public health, air quality control and environmental protection. Aerosolized NPs attract our attention because it can provide us the ideal model of well-suspended NPs. The electro spray technique can aerosolize particle droplets with minimal aggregation by controlling the electrical charge of the droplets, and thus form nano-sized particles for interacting with the cells. Using this method, we would like to examine the toxicity of aerosolized ZnO NPs using *E. coli* as the model microbial species. We will also study the toxicity of aerosolized ZnO NPs with

different sizes. This can help us to investigate the nano-associated toxicity and mechanism. The electrospray method will be applied to deliver several types of transition metal oxide (TiO₂, Fe₂O₃, NiO, CuO, and Co₃O₄) NPs to microbes for testing their eco-toxicity.

1.4.2. Systematically test ZnO NPs' eco-toxicity to different microorganisms.

We will test five model bacteria----Pathogenic bacteria (non-virulent species *Mycobacterium smegmatis*), metal reducing bacteria (*Shewanella oneidensis* MR-1), blue-green algae (*Cyanothece* 51142), yeast (*Saccharomyces Cerevisiae*) and enterobacteria (*Escherichia coli*). We would like to test the different cellular responses to NPs among five different microorganisms. This will help us to investigate the biological responses of different microbes to metal oxide NPs.

The main goal of this research is to address the mechanism of interaction between nano-sized metal oxide particles and microbes. We focus on the factors of microbial species, metal compositions, NPs' physical/chemical properties, and NPs' exposure modes. The anti-microbial activities of NPs can be explored for potential air purification applications, air quality control and public health (Ao and Lee 2005).

1.5 Outline of the thesis

Chapter 2 introduces the experimental materials and methods to study six types of transition metal oxide NPs and their interaction with different

microorganisms. Chapter 3 and Chapter 4 will introduce the results and discussions for the two different parts of researches. Chapter 5 is the conclusion of my thesis. The Appendix Project A and Project B contain my other two research works at Washington University. At the very end of the thesis I attached the references, acknowledgement and my Vita.

Chapter 2

Materials and methods for investigation of eco-toxicity of metal oxide NPs

2.1 Growth of cells with NPs in aqueous mode

Five microbial species were used in this study: one pathogenic bacterium (non-virulent species *Mycobacterium smegmatis*), one metal reducing bacterium (*Shewanella oneidensis* MR-1), one blue-green algae (*Cyanothece* 51142), one yeast (*Saccharomyces Cerevisiae*), and one enterobacterium (*Escherichia coli* strain BL21). *M. smegmatis* was grown in a Sauton liquid medium at 37°C (Tang et.al.2009); *S. oneidensis* MR-1 was grown in a MR-1 medium at 30°C (Tang et.al.2007); *E. Coli* were grown in a M9 medium at 37°C; *Cyanothece* 51142 was grown in a ASP2 medium at 30°C under continuous light ($50 \mu\text{mol photons m}^{-2}\text{s}^{-1}$) (Reddy et.al.1993); and *S. cerevisiae* was grown in a yeast synthetic-defined (SD) medium at 30°C. All cultures (50mL) were grown in flasks shaken at 150 rpm in the dark except *Cyanothece* 51142. ZnO (20 nm), ZnO (480 nm), and TiO₂ (20 nm) nanoparticles were obtained from NanoAmor (Houston, USA), and the NPs were dispersed in sterilized DI water to make 1 g/L solution. When the initial cell density in the cultures were equal to optical density (OD) ~0.1 (i.e. the early log phase), a certain amount of ZnO NP stock solution was added into cell cultures, and cell growth was monitored using a spectrometer (Genesys, Thermo Scientific, USA) at a wavelength of 600 nm (for *M. smegmatis*, *S. oneidensis* MR-1, *S. cerevisiae*, and *E. coli*) and 730 nm (for *Cyanothece* 51142). The tested NPs also

absorbed light at OD₆₀₀ and OD₇₃₀; thus the actual cell density was obtained based on:

$$OD_{\text{actual}} = OD_{\text{measured with NPs and cells}} - OD_{\text{measured with NPs in cell free solution}}$$

To test the toxicity of different metal oxide (TiO₂, NiO, ZnO, CuO, Co₃O₄ and Fe₂O₃) NPs, *E. coli* cells were used as the model microorganism. *E. coli* was cultivated in the M9 minimal medium at 37°C with glucose (2g/L) as the carbon source. The growth rates of *E. coli* culture (5mL, initial OD₆₀₀ =0.05) in the presence of NPs (particle size of 20 nm; 2, 20, and 100 mg/L) were monitored. In parallel, the experiments were also performed using soluble chloride salt of the metals (the ion concentrations were 2, 20, and 100 mg/L respectively) to test the metal ion's toxicity. Samples were taken after 2 hrs (in the early-log phase) and 8 hrs (in the middle-log phase) incubation. The inhibition rate from aqueous exposure was obtained based on the equation below:

$$Rate(\%) = \left[1 - \frac{OD(8h, stress) - OD(2h, stress)}{OD(8h, control) - OD(2h, control)} \right] \times 100\% \quad 2-1$$

2.2 Aerosol exposure of NPs to *E.coli*

An electrospray exposure system for NP dispersion was utilized to generate direct interaction between NPs and cells. Fig 2-1 shows the schematic diagram of the exposure system.

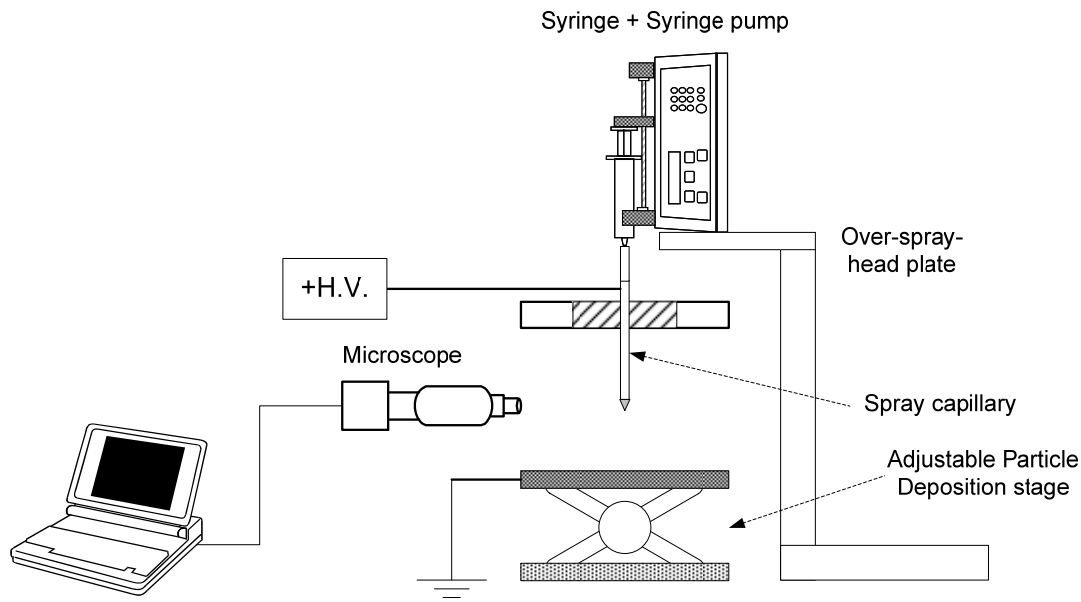


Figure 2-1 Electro spray experimental set-up

The system is composed of the electro spray head and particle deposition stage arranged in the point-to-plate configuration. The spray head consists of a single capillary which is installed at the top metal plate of the system. The electro spray device was carefully cleaned using 70% ethanol before all experiments. To generate the well suspended charged particles in the sprayed solution, a high voltage (7KV) of positive polarity was applied to the spray head and electrically grounded at the particle deposition stage where the samples were placed (the current through sample was limited to less than $0.2 \mu\text{A}$). The sprayed suspension was freshly prepared by dispersing NPs in a Na_2HPO_4 buffer solution with its electrical conductivity conditioned at 200-300 $\mu\text{S}/\text{cm}$ (Buffer solution at 25mM, pH=7.0; the buffer helped reduce NPs' aggregation during spraying). The suspension of NPs was fed into the spray capillary by a precision syringe, and its

flow rate ($\sim 5\mu\text{L}/\text{min}$) was controlled by a programmable syringe pump. During the electrospray process, charged individual particles formed a cone shaped spray and uniformly spread on the deposition stage.

In the aerosol exposure experiments, the aliquot of *E. coli* (total cell number $\sim 8 \times 10^8$) was first filtered onto a PVDF membrane ($0.22\mu\text{m}$ pore size, $1.25\text{cm} \times 1.25\text{cm}$, Millipore, US) to form a biofilm loosely attached to the membrane surface. The membrane was placed in the center of deposition stage and NPs were electrosprayed on the biofilm for 10 mins. After spraying of NPs (4 or 20 μg NPs were sprayed, equivalent to the concentration of 20 mg/L NPs or 100 mg/L NPs in a 0.2mL cell culture, respectively), the cells were washed from the membrane by vigorous vortex into 5mL of the minimal M9 medium. To measure the total number of living cells in this aqueous medium, a 0.1mL sample was taken and diluted before spreading on LB agar plates. Then the colony forming unit (CFU) was counted after the plates were incubated at 37°C for ~ 24 hrs. In parallel, the rest of solution was cultured on a shaker (250 rpm) at 37°C and the recovery of growth in the aqueous medium was monitored by OD_{600} . To study the ZnO NP toxicity via electrospray system, ZnO NPs (20 nm ZnO NPs and 480 nm ZnO NPs) or control solutions without NPs (sterile distilled water, 30 mg/L ZnCl_2 solution, or 25mM NaH_2PO_4 buffer solution) were electrosprayed onto the surface of the cell layer. The total exposure time was kept around 10 mins.

2.3 Analytical measurements

2.3.1 DNA release The release of intracellular DNA from cells in the presence of NPs was also investigated. The cells growing in the aqueous medium (with or without NPs) or washed from the membrane after electrospray were centrifuged at 4,000 rpm for 10 mins (4°C). DNA concentrations in these supernatant solutions (biological repeat, n=3) were measured using a spectrophotometer (Nanodrop, Thermo Scientific, USA) (Kang et al. 2008b). In order to determine the solubility of NPs in the aqueous environment, the concentrations of metal ions in the cultures were measured. NPs and cells were removed from the cultures by a high speed centrifugation (19,000×g) for 20 mins, after which the supernatant was collected and filtered (0.22 µm, Nylon, Millipore, USA). The ionic metal concentrations in the supernatants were determined at two different time points (2 hrs and 8 hrs, n=3) by Inductively Coupled Plasma Mass Spectrometry (ICP-MS, Agilent, USA).

2.3.2 GFP expression Expression of green fluorescent protein (GFP) by *E.coli* was measured to monitor the bacterial intracellular metabolic response to ZnO NPs' stress (Fan et.al.1996). The recombinant GFP-expressing *E. coli* (BL21 (DE)) was generated by cloning the GFP gene into a kanamycin-resistant pET30a (+) vector. 100 µM IPTG (Isopropyl β-D-1-thiogalactopyranoside, Fermentas, Canada) was added to the medium to induce the production of GFP after inoculation. The GFP production in GFP-expressing *E. coli* cells was monitored by a fluorescence reader (Bio-Teck, Vermont, USA) during growth. The

excitation wavelength was fixed within the range of 465 to 505 nm, and the emission wavelength was maintained between 508 and 548 nm.

2.3.3 EPS production The production of extracellular polymeric substances (EPS) from the surfaces of bacterial cells was measured (Liu et.al.2002; Zhang et.al.1999; Azeredo et.al.1999). The cells were cultured in the medium for 8 hrs (in the middle log phase) after inoculation. The dry biomass was determined by centrifuging down 200 mL microbial culture at 4,000 ×g for 15 mins (4°C) and drying cell pellets in an oven at 100°C overnight before weighting. The microbial floc was obtained by centrifuging 10 ml cell cultures at 4,000 ×g for 15 mins (4°C). After removing the supernatant, the microbial floc was dispersed into distilled water to keep the total volume at 10 ml. Then 12 µl formaldehyde (37%) was added and kept for 1 hr at 4°C; then 0.8 ml NaOH (1 N) was added and kept for 3 hrs at 4°C. The microbial floc solution was then centrifuged (13,200 ×g, 20 mins, 4°C) to remove the suspended solids before chemical component analysis. Polysaccharides and protein were dominant components in the extracted EPS. The polysaccharides concentration was determined according to the phenol-sulfuric acid method with glucose as a standard by using chromatography at 490 nm (Dubois et.al.1956). The protein concentration was determined by Bradford reagent using bovine serum albumin (BSA) as standard, which caused absorption maximum of the dye at 595 nm (Bradford et.al.1976).

2.3.4 Measurement of soluble ions In order to determine the solubility of NPs in the aquatic environment, we measured the concentrations of soluble ions in

different microbial culture solutions over time. Before the measurement, NPs and cells were removed from the culture by a high speed centrifugation ($19,000 \times g$) for 20 mins, after which the supernatant was collected and filtered ($0.22 \mu\text{m}$, Nylon, Millipore, USA). The ion concentrations in the supernatant at different time points (from 0~20 hrs, n=4) were determined by Inductively Coupled Plasma Mass Spectrometry (ICP-MS, Agilent, USA).

2.4 SEM and TEM protocols

Cell-free NP samples in the aquatic phase and the same samples created by electrospray process were obtained and deposited on the silicon wafers before drying in the air. The cell samples with NPs were deposited on a piece of membrane surface and fixed by adding 2% glutaraldehyde. After 2 hrs, the samples were washed in 0.10 M sodium cacodylate buffer for 20 mins three times. Then the samples were dehydrated in series of 10 mins washes in 50%, 70%, 85% and 95% ethanol and further were dried with freeze-drier equipment (Labconco, USA). A scanning electron microscope (SEM) (Nova 2300, FEI, USA) was used to image the samples. Additionally, a transmission electron microscope (TEM) was used to image cells exposed to NPs (20nm) in the aquatic phase. The NPs mixed with cells were centrifuged down and fixed in 4% Paraformaldehyde / 2.5% Gluteraldehyde in a 0.1M cacodylate buffer (pH 7.2) overnight. Samples were treated with Osmium Tetroxide and were dehydrated using ethanol before they were embedded into Pelco Eponate 12 resin (Ted Pella Inc., Redding, USA). Sections of the samples were cut on an Ultramicrotome (Leica, Germany),

inspected in the TEM (H7500, Hitachi, Japan) at 80 kV using the HR mode, and photographed by a digital camera (Hamamatsu, Japan). Meanwhile, *E. coli* cells in the aqueous medium were also observed under light microscopy (LEICA DM4000B) during their growth.

Chapter 3

Results and discussion for investigation of eco-toxicity of for six types of transition metal oxide NPs

3.1 Effect of metal oxide NPs on microbial growth

It has been well known that ions of some transition metals display toxic characteristics toward biological systems. Table 3-1 indicates that the tested ionic species inhibit *E. coli* growth when ion concentrations are above 20 mg/L: Ni^{2+} , Co^{2+} , Zn^{2+} , and Cu^{2+} show high inhibition rates to microbial growth, while Fe^{3+} has relative low toxicity. However, the tested metal oxide NPs (TiO_2 , ZnO , CuO , Co_3O_4 and Fe_2O_3) appear to be non-toxic to *E. coli* at the low concentration (2 mg/L), and they also exhibit insignificant toxicity to *E. coli* even at concentrations as high as 20 mg/L and 100 mg/L. Interestingly, NiO NPs show the high growth inhibitory effect at the concentrations of 20 mg/L and 100 mg/L (34% and 85% respectively) although a negligible effect occurs at the low concentration of 2 mg/L. It has been confirmed in our previous study (Wu B et.al.2010a) that the antimicrobial activity of metal oxide compounds in aquatic system was mainly caused by soluble ions. This is because the NPs often aggregate in the aqueous medium; their nano-associated particle effect on cellular function is reduced.

Table 3-1. Responses of *E. coli* to NPs and metal ions in the aqueous phase

		<i>NiO</i> (<i>Ni</i> ²⁺)	<i>ZnO</i> (<i>Zn</i> ²⁺)	<i>Fe</i> ₂ <i>O</i> ₃ (<i>Fe</i> ³⁺)	<i>Co</i> ₃ <i>O</i> ₄ (<i>Co</i> ²⁺)	<i>CuO</i> (<i>Cu</i> ²⁺)	<i>TiO</i> ₂
Metal Ions (mg/L)	2	7±12	7±9	-22±5	1±4	13±10	NA
	20	34±9	12±10	-15±10	50±9	67±12	NA
	100	85±4	38±9	-11±6	80±7	78±5	NA
NPs (mg/L)	2	14±5	1±9	5±9	-8±21	2±7	0±5
	20	30±7	21±15	-16±24	-11±12	8±12	-6±23
	100	46±10	9±22	-11±25	0±15	27±13	8±9

NA: not applicable

Table 3-2. Release of metal ions (mg/L) from metal oxide NPs (20 mg/L) in the aqueous phase

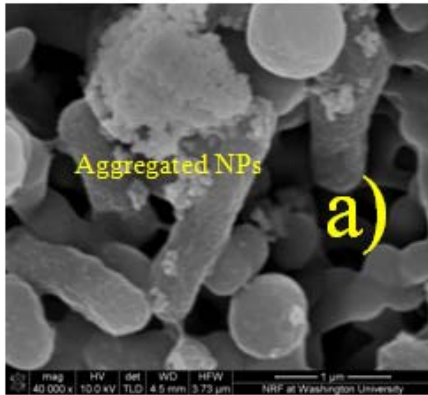
Sampling times	<i>NiO</i>	<i>ZnO</i>	<i>Fe</i> ₂ <i>O</i> ₃	<i>Co</i> ₃ <i>O</i> ₄	<i>CuO</i>	<i>TiO</i> ₂
2hr	0.27±1	2.44± 0.23	0.07±0	0.02±0	0.51±0.02	ND
8 hr	0.49±0.02	2.71 ±0.91	0.09±0.03	0.02±0	1.5±0.17	ND

ND: not detectable

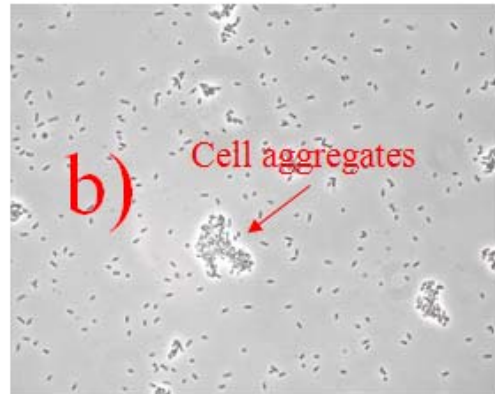
The solubility data (Table 3-2) reveals that NiO, ZnO and CuO NPs (20 mg/L) release 0.5~2.7 mg/L metal ions in the aqueous system during the culture period (8 hrs). At this concentration level, the three NPs have relatively low toxicity in the aqueous medium (10~30% inhibition rate). Also, a recent study (Horie et.al. 2009) shows that extracellular nickel ions cannot easily pass through the cell membrane via ion channels, but small nickel particles can be uptaken by cells and then release Ni²⁺ intracellularly. On the other hand, Co₃O₄ and Fe₂O₃ have very low solubility, so they cannot inhibit *E. coli* growth.

3.2 Effect of aerosolized metal oxide NPs on microbial survival

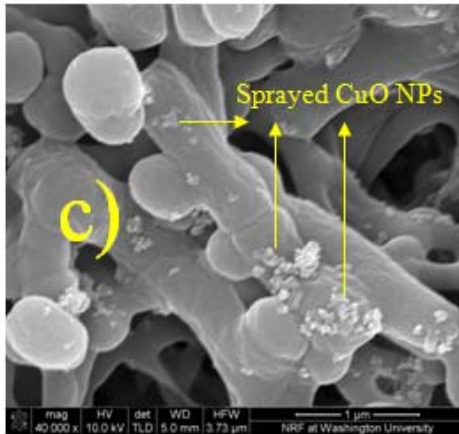
Metal oxide NPs in the aqueous medium display different solubility and the dissolved metal species can provide a possibility for NPs to aggregate in the aqueous system. This phenomenon can lead to the limited availability of particles to bacteria (i.e. ineffective interaction) (Fig 3-1a).



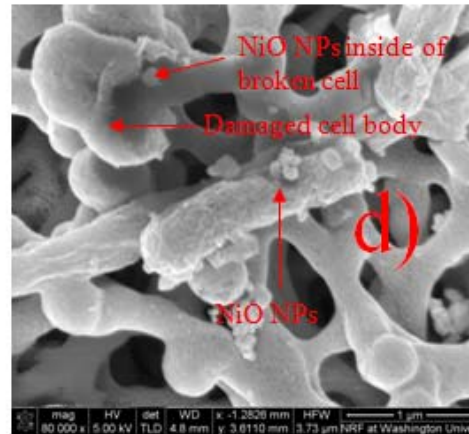
With NiO NPs in aqueous solution



Stressed *E. coli* with Cu²⁺



After electro spraying CuO NPs



After electro spraying NiO NPs

Figure 3-1. SEM images of *E. coli* with NPs

In this study, the employed “electrospray” technique provides a new approach to disperse NPs in their original sizes, allowing direct interaction between NPs and bacteria (an *E. coli* biofilm layered on a membrane surface).

Table 3-3. Percentage (%) of *E. coli* viability reduced after exposure to aerosolized metal oxide NPs (comparing to exposure to particle free buffer solution)*

	NiO	ZnO	Fe₂O₃	Co₃O₄	CuO	TiO₂
4 µg	45±16	52±16	-21±23	12±22	35±4	19±24
20 µg	88±5	71±19	-12±14	5±14	77±11	21±19

*: viability reduced rate = 100% - CFU_(after exposure with NPs) / CFU_(after exposure with buffer solution)

Table 3-3 shows the percentages of reduced bacterial viability based on the total living cell number by counting CFU after aerosol exposure of NPs. It is apparent that NiO, CuO and ZnO NPs significantly reduces viability of *E. coli* even with a short exposure time (10 min) (spray amount of 4 µg NPs) compared to the control (electrospraying buffer solution only): viable cells were reduced by 45% for NiO NPs, 52% for ZnO NPs and 35% for CuO NPs. Increasing the spray dose up to 20 µg of metal oxide NPs can further enhance NP lethality to bacteria: viable cells are reduced by 88% for NiO NPs, 71% for ZnO NPs and 77% for CuO NPs. However, less soluble Co₃O₄ and non-soluble TiO₂ NPs display low toxic effects on *E. coli* after electrospray (viability reduced less than 20%). Fe₂O₃

NPs show no antimicrobial activity under the all tested conditions: soluble metal ion, aqueous solution, and aerosol exposure. Also, after direct spraying the NPs onto bacteria and immediately transferring cells into the liquid medium, the growth recovery from NiO NP-sprayed samples is much slower than the other samples (Fig 3-2).

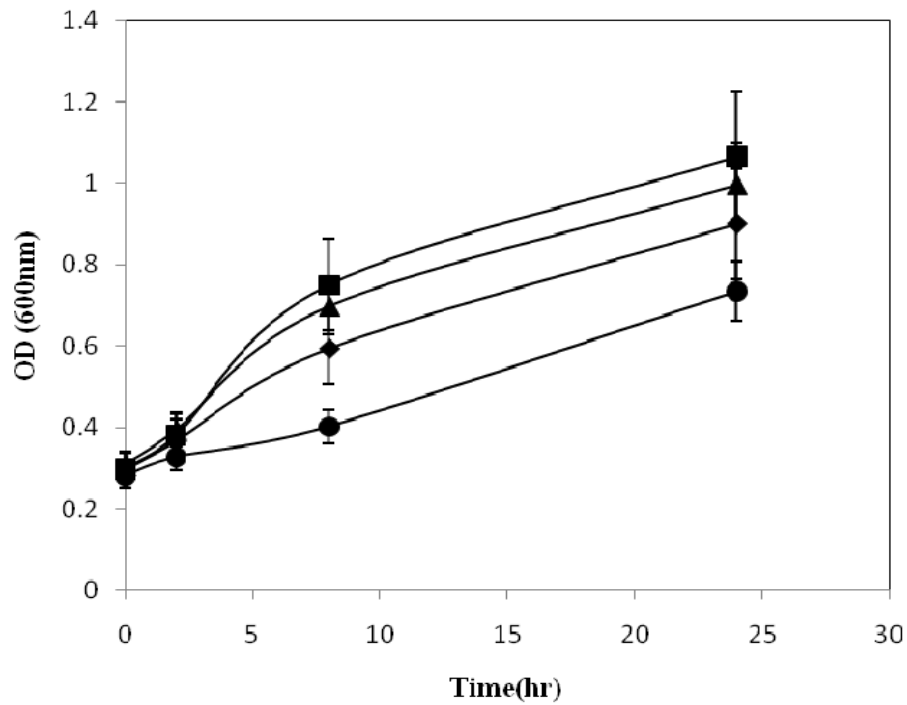


Figure 3-2. The growth recovery of *E.coli* in a M9 minimum medium after electro spraying transition metal oxide NPs (20 μ g) (n=3); (□) After electro spraying buffer; (Δ) After electro spraying TiO₂ NPs; (◇) After electro spraying CuO NPs; (○) After electro spraying NiO NPs.

3.3 Mechanisms of metal oxide NPs' antibacterial activities

In the aqueous phase, the antibacterial activities of metal oxide NPs are mainly due to metal ions released from nano-sized particles. Therefore, the solubility of metal oxide particles and the toxicity of metal ions can be considered as two key factors for evaluating NPs' antimicrobial activities. For example, among all the six tested types of NPs, NiO NPs show the highest antimicrobial activities, though its solubility in the aqueous culture medium is lower than CuO or ZnO NPs. This is consistent with the fact that Ni²⁺ has the highest toxicity to cells (Table 4-1). The small particle size of NiO could enhance its solubility and the presence of extracellular Ni²⁺ could interfere with the intracellular Ca²⁺ metabolism and cause cellular damage (Horie et al. 2009).

On the other hand, due to the dissolving properties of NPs in the aqueous environment, NPs tend to aggregate; thus the direct interaction between particles and bacteria is limited (Wu B et al. 2010a). Meanwhile, *E. coli* cells appear to aggregate under the effect of antimicrobial reagents because environmental stress (such as acids, toxic metal ions, and lack of nutrients) could trigger protein misfolding and cellular aggregation (Kwiatkowska et al. 2008). For example, our previous work show that *E. coli* cells aggregate when they are exposed to soluble toxic metal ions (16 mg/L ionic Cu²⁺) (Fig 3-1b). Therefore, the NPs' antimicrobial activity in the aqueous phase is reduced. However, the aerosol exposure mode via the electrospray technique could significantly enhance the interaction between NPs and bacteria by uniformly distributing NPs on bacterial

surface (Fig 3-1c). The SEM pictures also show that NiO NPs cause the direct damage of cellular structures (Fig 3-1d), which probably lead to the lysis of the cells. Furthermore, the release of DNA molecules from bacterial lysis could be an indicator of cellular structure integrity. After exposure to aerosolized NPs, bacteria were washed into the liquid medium and the total nucleic acids in the supernatant was 12 $\mu\text{g/L}$ after NiO exposure (20 μg), which is higher than 8 $\mu\text{g/L}$ after CuO exposure (20 μg) (Table 3-4). This observation further supports that NiO NPs may interact with *E.coli* cells more efficiently than other types of NPs do (Horie et al. 2009). Therefore, metal oxide NPs' biological effects could be derived from (1) the locally concentrated ion zone formed by release of metal oxide NPs; and (2) the nano-related stress from nanoparticles on cellular structure integrity.

3.4 Biological responses and dissolution of transition metal oxide NPs

The biological responses to Metal Oxide NPs were further explored at the molecular level. EPS (mainly consist of polysaccharides, proteins, lipids, and also a component of nucleic acids and other bio-polymers) are excreted by many microorganisms. Due to the properties of EPS, they could cause a barrier to reduce interaction between the cells and NPs or toxic chemicals. Cells could produce extracellular substances, which contain the released intracellular DNA. We measured the released intracellular DNA in solution to determine the cellular response to the stress of NPs.

Table 3-4: Released DNA in the aqueous phase (20 mg/L) and after electro-spraying and solubility in the aqueous phase (20 mg/L)

			Control	NiO	ZnO	Fe ₂ O ₃	Co ₃ O ₄	CuO	TiO ₂
In the aqueous Phase (µg/L)	2h	DNA	14±0.5	8±1	13±1	13±1	9±4	10±4	8±4
	8h	DNA	26±1.5	16±2	24±2	29±6	31±2	24±3	27±3
After Electro-spray (µg/L)	DNA		11±4.6	4±2*	-	-	-	10±4*	-
	DNA			12±1**	-	-	-	8±7**	-

* The amount of metal oxides was electro-sprayed was equivalent to 4 µg;

** The amount of metal oxides was electro-sprayed was equivalent to 20 µg;

In Table 3-4 we can find that in aquatic system, the amount of released DNA of the cells under NPs' stress doesn't have significant difference from the amount of released DNA of the control cells. This result is consistent with the toxicity of NPs in aqueous solution, which indicates that the toxicity for NPs in aqueous solution is mainly attributable to the dissolved ions, and due to the low solubility for these transition metal oxide NPs, their toxicity in aquatic system is not significant.

For the "aerosol exposure" under the "electrospray", we also measured the amount of released DNA for CuO and NiO NPs soon after the NPs electro-sprayed onto the biofilm. We can find that the DNA release of the cells under NiO and CuO NPs' stress is not significant. For high dose NiO NPs, the amount of released DNA of the cells under NPs' stress is slightly higher than the amount of released

DNA of the control cells, which indicates that NiO NPs with high dose might make some physical damage to the cells. The reason might be due to the synergistic effect of NPs' toxicity to the *E.coli* cells. The locally concentrated ionic species as well as mechanical stress are two main reasons for NPs' toxicity to *E.coli* cells. Released intracellular DNA is just a small part of EPS, judging the amount of released DNA can be only used as a reference for NPs' stress to *E.coli* cells. There might be other biological techniques which can verify the interactions between NPs and the cells.

Chapter 4

Results and discussion for extensive investigation of ecotoxicity of ZnO NPs to different microorganisms

Now we focus on ZnO NPs toxicity to different microorganisms. We have also tested the factors affecting ZnO NPs' interaction with microbes. This work has been published (Wu B et.al. 2010b) and I am one of the authors for this publication. The following discussion consists part of my MS thesis work.

4.1 Effect of ZnO NPs on microbial growth in aquatic exposure mode

Table 4-1 displays the different growth responses of microorganisms to ZnO NPs (20 nm) in the aquatic medium. ZnO NPs apparently inhibit the growth of *M. smegmatis* and *Cyanothece* 51142 in a dose response manner. Initial bacterial population also affects their response to ZnO NPs. When the initial cell density, prior to the NPs' stress, is reduced from 0.1 to 0.01, the sensitivity of the response is magnified (Fig 4-1). It is apparent that *M. smegmatis* growth (initial OD ~ 0.01) is significantly reduced by ZnO NPs as low as 0.2 mg/L. This observation is consistent with the results of the previous experiment, in which we found that the initial bacterial density was closely related to bacterial resistance to NP stress, an increase of cell population could alleviate the inhibitory effect from toxic NPs (Wu B et.al. 2010a).

Table 4-1. Inhibition to microbial biomass production (initial OD₆₀₀=0.1) and GFP production of *E. coli* in the presence of ZnO NPs (n=3).(Wu B et.al.2010b)

Species	Inhibition rates (%) in presence of ZnO NPs or Zn ²⁺ *				Inhibition of growth in presence of ZnO NPs (20 mg/L) after adding EDTA (60 mg/L) (%)		Inhibition of GFP production by ZnO NPs (%)
	NPs (mg/L)			Zn ²⁺ (mg/L)	EDTA only	EDTA +NPs	
	2	20	40	16			
<i>S. oneidensis</i>	9±8	11±6	3±13	10±6	-	-	-
<i>M. smegmatis</i>	18±11	38±8	60±19	48±18	16±4	17±5	-
<i>Cyanothece</i> 51142	7±16	69±16	74±19	75±19	-	-	-
<i>S. cerevisiae</i>	-3±3	-2±6	-1±2	-6±8	-	-	-
<i>E. coli</i>	1±5	6±10	3±6	2±5	-	-	-2±3 ¹ 10±7 ²

* Inhibition rates were calculated based on the cell densities obtained from different culture conditions. The OD was measured after culturing all microbial species to the late exponential growth phase:

$$rates (\%) = \left\{ 1 - \frac{OD(stress\ condition)}{OD(control\ condition)} \right\} \times 100\%$$

1. 20 mg/L ZnO NPs
2. 60 mg/L ZnO NPs

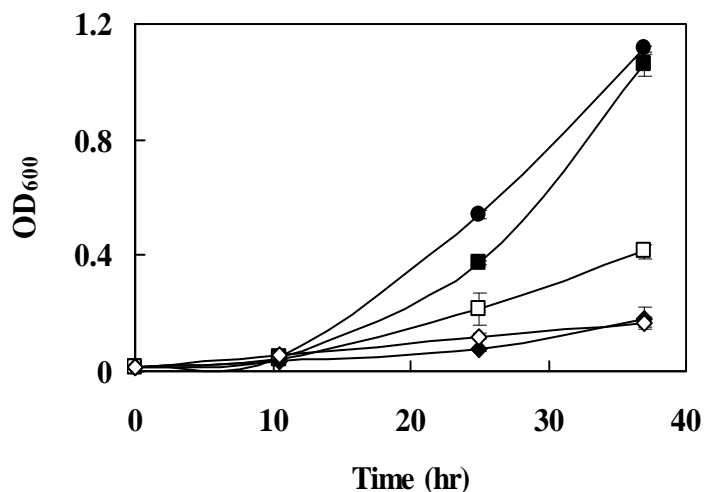


Figure 4-1. Sensitivity of *M. Smegmatis* (initial $OD_{600}=0.01$) to the dose of ZnO NPs (20 nm). (●) control; (■) 0.2 mg/L; (□) 0.5 mg/L; (◆) 2 mg/L; (◇) 20 mg/L. Error bars were the standard deviations (σ) of the replicate analyses.(Wu B et.al.2010b)

However, ZnO NPs (up to 40 mg/L) or 16 mg/L Zn^{2+} do not suppress the growth of *S. oneidensis*, *S. cerevisiae* or *E. coli* (Table 4-1). Normally, Daphnia species has been used to assess Zn^{2+} toxicity (based on the mortality of Daphnia species after one week of exposure) (Tang et.al.2009), but our study shows that zinc toxicity could be more quickly assessed by *M. smegmatis* in 1-2 days.

ZnO NPs are slightly soluble in an aquatic medium, the measured average Zn^{2+} concentration was $\sim 2.6 \pm 0.8$ mg/L in all culture medium (pH \sim 7.0; ZnO NPs =20 mg/L). For example, in the *E. coli* culture, Zn^{2+} concentration was 2.4 ± 0.4 mg/L at an early growth phase (0~4 hrs); but was 2.7 ± 0.7 mg/L at a late growth phase (after 15 hrs). This result indicates that ZnO NPs can serve as a Zn^{2+} carrier and maintain a relative constant Zn^{2+} concentration in the aquatic solution. The previous studies of ZnO NPs using microalgae as a model microorganism point

out that Zn^{2+} ions dissolve from ZnO are the primary cause for ZnO ecotoxicity (Aruoja et.al. 2009), so the toxicity of both ZnO bulk material and ZnO NPs are comparable to that of $ZnCl_2$ (Franklin et.al. 2007). Such result is also observed in this study. For example, when $ZnCl_2$ was added into culture medium (Zn^{2+} equal to 16 mg/L, equivalent to total zinc in 20 mg/L ZnO), the similar growth inhibition rate as that of 20 mg/L ZnO NPs was observed for *M. smegmatis* (Table 4-1). However, if we supplement 60 mg/L EDTA (a chelating agent) to the culture medium to deactivate Zn^{2+} , the inhibition of *M. smegmatis* growth caused by ZnO NPs (20 mg/L) was significantly alleviated (inhibition rate dropped from 38% to 17%) comparing to the control samples.

EPS (mainly polysaccharides and proteins) are excreted by many microorganisms, and are normally attached to the cell surface, which build up a barrier to protect cells (Liu et.al. 2002). Table 4-2 shows that *M. smegmatis* and *Cyanothece* 51142 contained little extracellular protein during their exponential growth phase (Trabelsi et.al. 2009). In comparison, *S. oneidensis* MR-1 and *E. coli* were able to produce significant amount extracellular protein (Eboigbodin et.al. 2008). Such extracellular protein may bind Zn^{2+} and reduce the interaction between cells and the NPs, so that *S. oneidensis* MR-1 and *E. coli* could grow normally in the presence of ZnO NPs (Panoff et.al.1988; Sutherland et.al. 2001; Teitzel et.al.2003; Wolfaardt et.al.1994). The fact that ZnO NPs did not interfere with *E. coli* intracellular functions were further confirmed by GFP-expressing recombinant *E. coli* (Tsien et.al.1998; Gogoi et.al.2006). When the concentration of ZnO NPs was raised up to 60 mg/L, intracellular protein GFP synthesis by *E.*

coli was minimally affected ($10 \pm 7\%$) (Table 4-1). This result indicates that some environmental bacteria have evolved excellent mechanisms to protect themselves from NP stresses while maintaining their normal intracellular functions.

Table 4-2. EPS production under the stress of ZnO NPs (20 nm, 20 mg/L) during the exponential growth phase (n=3). (Wu B et.al.2010b)

		Protein	Polysaccharides
		(mg/g dry biomass)	(mg/g dry biomass)
<i>S. oneidensis</i>	Control	45±14	53±7
	With NPs	58±16	48±11
<i>M. smegmatis</i>	Control	<1	23±12
	With NPs	<1	29±8
<i>Cyanothece</i> 51142	Control	<1	21±10
	With NPs	<1	38±11
<i>S. cerevisiae</i>	Control	2±2	72±13
	With NPs	2±1	75±19
<i>E. coli</i>	Control	32±9	63±15
	With NPs	50±23	69±16

* The enhancement of microbial protein productions by ZnO nanoparticles were not statistically significant (*S. oneidensis*, P value = 0.19; *E. coli*, P value = 0.13); Also, the differences of microbial polysaccharides productions between without ZnO nanoparticles and with ZnO nanoparticles were not statistically significant (*S.*

oneidensis, P value = 0.24; *M. smegmatis*, P value = 0.20; *Cyanothece* 51142, P value = 0.19; *S. cerevisiae*, P value = 0.29; *E. coli*, P value=0.10).

4.2 Aerosol exposure of ZnO NPs to cells using electrospray

ZnO NPs showed severe aggregation in the aquatic medium (Fig 4-2A, C), resulting in the formation of flocs of variable sizes up to several microns in diameter (Adams et.al.2006; Aruoja et.al.2009; Franklin et.al.2007; Auffan et.al.2009; Wang H.H. et.al. 2009). These aggregates restricted the particles' interaction/uptake by viable *E. coli* (Limbach et.al. 2005; Thill et.al. 2006; Schipper et.al. 2005). Our results also indicated that different primary sizes of ZnO NPs (20 nm and 480 nm) displayed the same level of inhibition to the growth of all tested microorganisms in the aquatic medium, which was similar to the observation by other researchers (Franklin et.al. 2007). Therefore, the toxicity of ZnO NPs was mainly associated with dissolved zinc species in the aquatic exposure mode. In this study, we demonstrated that in bacterial exposure to ZnO NP aerosol, the NPs' antimicrobial activity could be significantly different from that in the aquatic environment. Via the electrospraying, NPs were uniformly dispersed onto a silicon wafer (Fig 4-2B). This technique was used to aerosolize NPs and to directly spray ZnO particles on bacterial surface, where a layer of *E. coli* cells was deposited on a membrane surface (Fig 4-2D). Based on the number of total viable *E. coli* colony counted (CFU data, Fig 4-3) after electrospray of NPs, ZnO significantly reduced the viability of *E. coli* even with a short exposure time (10 min).

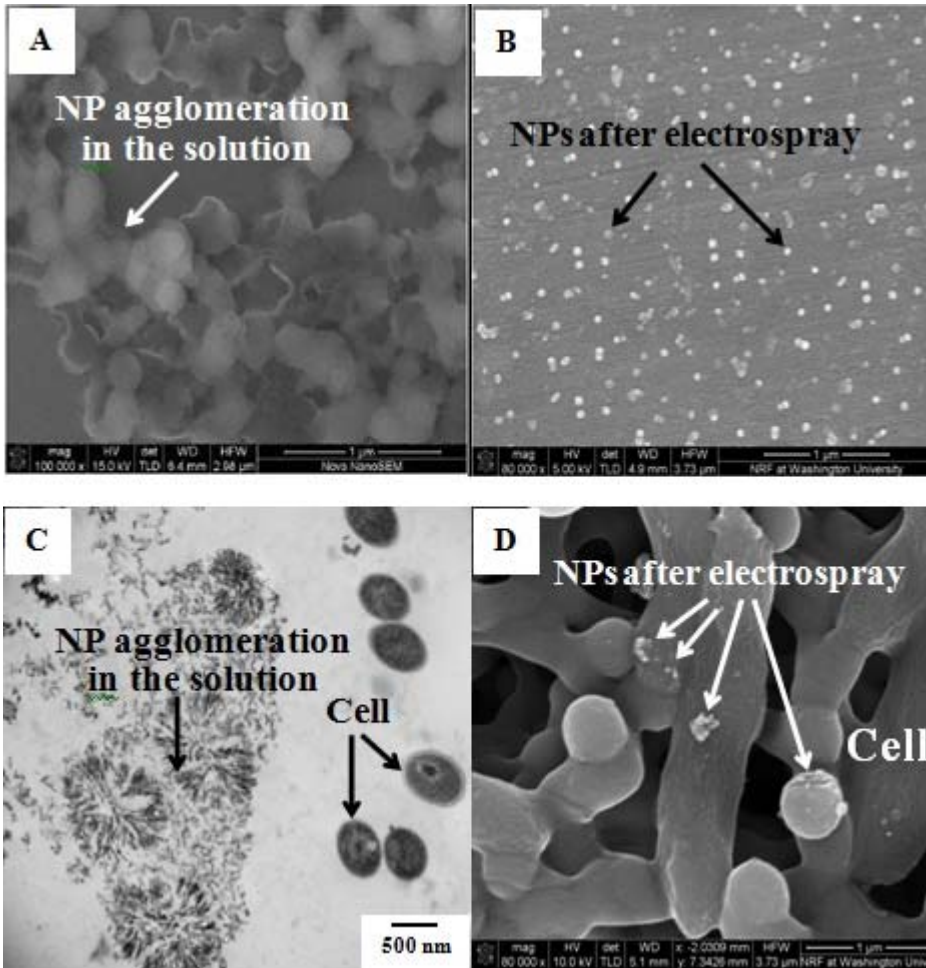


Figure 4-2. SEM and TEM images of ZnO NPs (20 nm) and ZnO NPs with bacterial cells. (A) ZnO NPs in the aquatic medium (pH 7.0); (B) ZnO NPs after electrospray; (C) ZnO NPs (20 mg/L) with bacteria (*M. smegmatis*) in the aquatic medium; (D) Aerosol exposure of ZnO NPs on bacterial surface (*E. coli*). (Wu B et.al. 2010b)

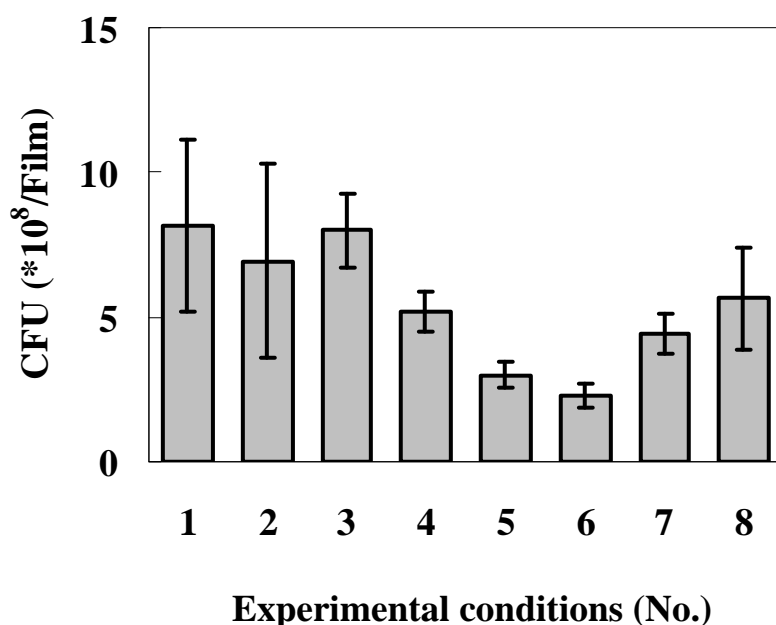


Figure 4-3. Investigation of toxicity after *E. coli* was electrospayed with NPs (n=3) (1) initial viable *E. coli* deposited on the membrane; (2) viable *E. coli* after electrospaying water (without NPs); (3) viable *E. coli* after electrospaying 30 mg/L ZnCl₂ solution (total 3.2 μg Zn²⁺); (4) viable *E. coli* after electrospaying buffer (as the control experiment); (5) viable *E. coli* after electrospaying buffer with ZnO NPs (20 nm, 4 μg), P-value=0.002; (6) viable *E. coli* after electrospaying buffer with ZnO NPs (20 nm, 20 μg), P-value=0.01; (7) viable *E. coli* after electrospaying buffer with ZnO NPs (480 nm, 4 μg), P-value=0.01; (8) viable *E. coli* after electrospaying buffer with TiO₂ NPs (20 nm, 4 μg), P-value=0.19. (Wu B et.al. 2010b)

Total viable cells on the membrane dropped from 6.9×10^8 (after electrospaying buffer solution) to 3.0×10^8 (after electrospaying 4 μg 20 nm ZnO NPs). Compared to the control experiments (n=3, electrospaying buffer solution only), such reduction of viable *E. coli* (~57%) was statistically significant (P-value=0.002; the P-value was calculated via two-sample T-test). Further

increasing the dose of ZnO NPs spray from 4 to 20 μg could reduce viable *E. coli* by more than 72% compared to the same control experiments (Fig 4-3) (P-value=0.01). This result revealed that ZnO NPs clearly led to the lethality of *E. coli* due to their specific nano-scaled characteristics (e.g. greater surface area).

On the other hand, electrospray of ZnO NPs with particle sizes of 480 nm caused less toxicity than 20 nm ZnO NPs, lowering the viable *E. coli* by 36% (P-value=0.01). Meanwhile, when 30 mg/L ZnCl_2 solution (total 3.2 $\mu\text{g Zn}^{2+}$, equivalent to 4 $\mu\text{g ZnO}$) was electrosprayed onto the *E. coli* biofilm, the total number of viable cells ($\sim 7 \times 10^8$) on the membrane was not apparently reduced (compared to the experiments with electrospraying buffer solution or sterile water). This indicates that ZnO NPs are more toxic than Zn^{2+} if they fully interact with cells. Also, insoluble TiO_2 NPs (20 nm) displayed much less toxic effect than ZnO NPs to *E. coli* under aerosol exposure mode (TiO_2 caused a decrease of cellular viability by $\sim 20\%$; however, error bars in Fig 4-3 indicate that the difference was not statistically significant, P-value=0.19). Interestingly, after spraying with NPs and immediately transferring the cells from the membrane to the liquid medium, we found that the *E. coli* cells were able to recover their growth rate back to normal levels with an apparent lag phase (>3 hrs, Fig 4-4) (comparing to the control experiments in aquatic mode).

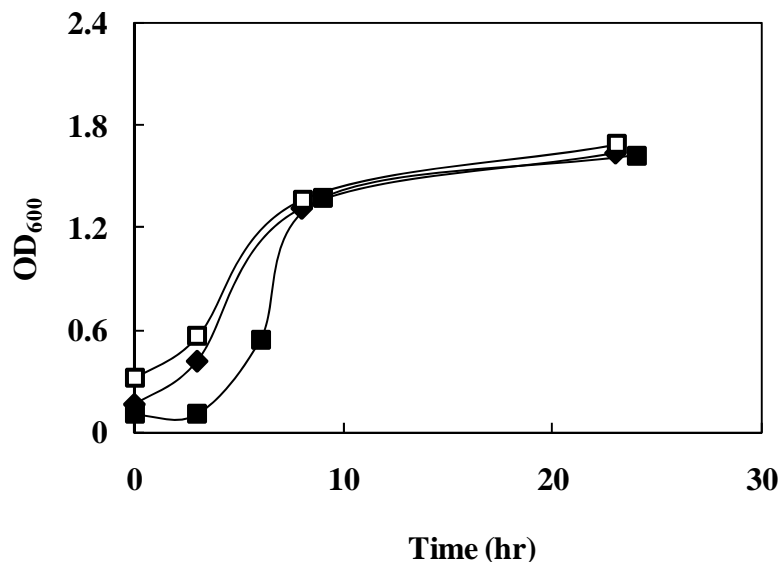


Figure 4-4. Growth curves of *E. coli* in the aquatic medium (n=3) (□) *E. coli* in the aquatic medium without ZnO NPs; (◆) *E. coli* in the aquatic medium with ZnO NPs (100 mg/L, 20 nm); (■) *E. coli* cells were transferred from the membrane to liquid medium after electro spraying ZnO NPs (4 μg, 20 nm). (Wu B et.al. 2010b)

This observation indicated that the stress of ZnO NPs was eventually removed once *E. coli* cells were exposed to an aquatic solution. The SEM image shows that the electro spray process significantly reduced ZnO NP aggregation and nano-size particles were resided on bacterial surface, although electro spray technique could not completely avoid a local and unequal distribution of particles on cell membrane because of an irregular surface of the biofilm (Fig 4-1D). After ZnO NPs were electro sprayed, the individual NPs or small-sized aggregated particles were tightly attached on the cellular surface, which may serve as a Zn²⁺ carrier and enhance the transport of toxic Zn²⁺ across cellular protective “barriers”

(such as EPS and cell walls). Therefore, the ZnO NPs' anti-microbial activity, resulting from the aerosol exposure process, was enhanced by the synergistic influence of particle's physical effect combined with the Zn²⁺ stresses.

Chapter 5

Conclusion and acknowledgements

5.1 Conclusion

This study compares two exposure modes for ZnO NPs' toxicity, as well as the other five types of transition metal oxide NPs' toxicity (NiO, CuO, Fe₂O₃, TiO₂, and Co₃O₄). Researchers have previously shown that under the aquatic exposure mode, NPs can be more toxic to cells than the metal ionic species at the corresponding concentration. This can be explained by a nano-trojan horse type of mechanism where the particles dissolve intracellularly (Limbach et.al. 2007).

ZnO NPs are not likely to be taken up by bacteria (in contrast to mammalian cells in culture). ZnO NPs' toxicity is mainly controlled by Zn²⁺ due to particle aggregation in the aquatic phase. Microbial species, sensitive to the Zn²⁺, are also sensitive to ZnO NPs. *M. smegmatis* growth will be inhibited by both ZnO NPs and Zn²⁺ in aquatic phase. On the other hand, direct exposure of ZnO NPs to *E.coli* cells via electrospray technique results in a significantly higher antimicrobial activity. This phenomenon is due to both the cells' physical damage by NPs and dissolved Zn²⁺ stress to the cells. Size effect of ZnO NPs is apparent for aerosolized NPs' toxicity: larger particles cause less toxicity or lethality to bacteria while smaller particles cause more toxicity to the *E.coli* cells. This observation indicates that aerosolized NPs can be potentially used as antibacterial reagents.

As for the other five types of transition metal oxide NPs in the aqueous system, both NPs and stressed bacteria tend to aggregate and the NPs' toxicity mainly attributes to the dissolved ions in solution. However, the antimicrobial activity of NPs is much higher under the aerosol exposure mode, which is consistent with the observations for ZnO NPs. NPs appear to display the synergistic effect of antimicrobial activities by both soluble ion stress and the particles' nano-related stress. Among the tested types of transition metal oxide NPs under both aqueous exposure and aerosol exposure modes, the observed antimicrobial activity is ranked as: NiO > ZnO \approx CuO > TiO₂ \approx Co₃O₄ \approx Fe₂O₃. NP composition, solubility and interaction modes with biological systems can be considered as the three main factors for risk assessment of metal oxide NPs.

5.2 Acknowledgements

This work was performed in part at the Nano Research Facility (NRF), a member of the National Nanotechnology Infrastructure Network (NNIN), which is supported by the National Science Foundation under NSF award No.ECS-0335765. This study was also supported by I-CARES and MAGEEP at Washington University in St. Louis and by the DOD-MURI Grant, FA9550-04-1-0430. The author gives the sincere gratitude to his advisor, Professor Yinjie Tang, as well as Professor Da-Ren Chen, Professor Young-Shin Jun, Cynthia Lo and Professor Younan Xia for their great help and supervision for my MS thesis research.

Appendix

Besides my MS thesis research about eco-toxicity for transition metal oxide NPs, I also did two independent research works with Professor Younan Xia and Professor Young-Shin Jun, respectively. The two independent studies all resulted in publications. I will introduce the two independent researches briefly at the very end of my MS thesis.

Project A

Probing the Photothermal Effect of Gold-Based Nanocages with Surface-Enhanced Raman Scattering (SERS) (advisor: Professor Younan Xia and Professor Cynthia Lo)

Surface-enhanced Raman scattering (SERS) is a fascinating process by which normally weak Raman signals can be amplified by 8–10 orders in magnitude. These large enhancements are mainly caused by the strong, light-induced electromagnetic fields (E-fields) at the surface of a metallic nanostructure. The superb sensitivity of SERS has shaped the mainstream view of this method as one primarily to be implemented for trace detection. SERS can reveal the structural information of molecules adsorbed on the surface of an Au or Ag nanoparticle. These surfaces continue to gain importance as nanoparticle engineering and surface functionalization become ever more sophisticated to meet the demands of new applications. One application where this surface plays a pivotal role is the photothermal (PT) effect. The PT effect occurs when a metal nanoparticle absorbs light and releases it as heat. This heat can affect the molecules on the nanoparticle's surface and heat up the local environment, both

of which have been actively exploited for drug delivery, cancer therapy, and lithography applications.

No one has actually quantified the Photothermal (PT) effect. Although it is still a challenging task, we attempted to build up the simple model to quantify the PT effect with SERS. The Self-Assembled Monolayers (SAMs) are exploited as a simple tool in our research. 1-dodecanethiolate (1-DDT) molecules are chemisorbed onto the surface of Au-based nanocages. We tested the structural changes in three different temperatures via SERS, as well as molecular dynamic (MD) simulations. The fundamentals of SERS and PT effect are quite similar, they all caused by Plasmon excitation that generates strong local E-field for SERS and heat for PT, respectively. SERS provides an effective approach for probing the PT effect without the sophisticated equipments or methods.

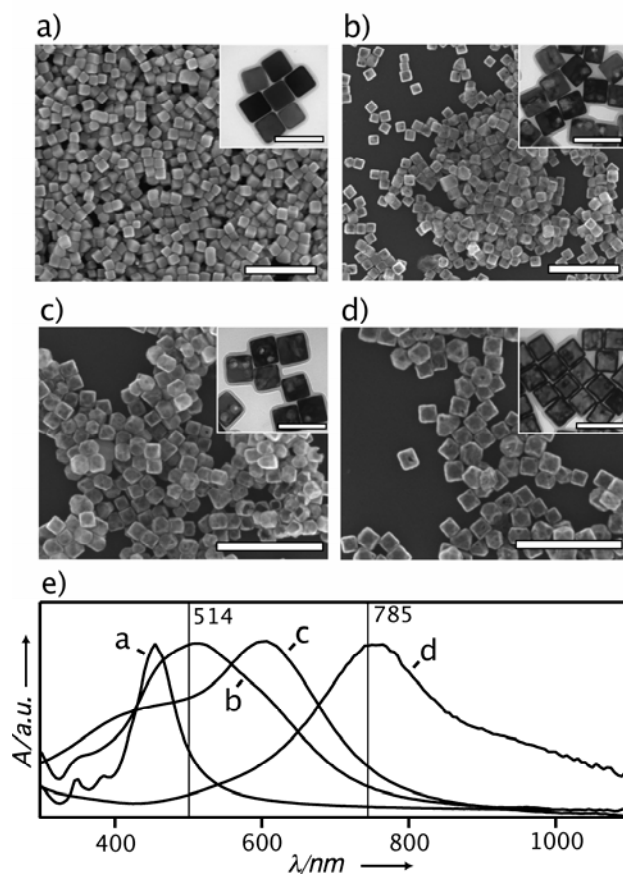


Figure A-1. SEM and TEM images of the Ag nanocubes (a) and the Au-Ag nanocages (b-d) used in this study. The scale bars are 500 nm and 100 nm for SEM and TEM (inset) images respectively. (e) Absorbance spectra of the nanocubes and nanocages. The nanocages were prepared from the nanocubes in (a) via the galvanic replacement reaction and their LSPR was tuned to 525 nm (b), 620 nm (c), and 790 nm (d). The vertical lines in (e) correspond to the wavelengths of the excitation sources used in this experiment. (M.Rycenga and Zhipeng Wang et.al. 2009)

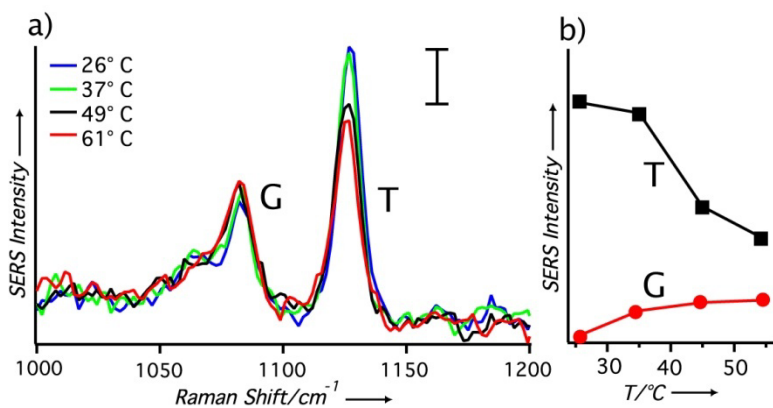


Figure A-2. (a) The SERS spectrum of aqueous 1-DDT nanocubes at different solution temperatures with 514 nm excitation. The temperature of the solution was controlled with a temperature control stage. The spectrum contains the gauche (G) 1080 cm⁻¹ and trans (T) 1125 cm⁻¹ carbon-carbon stretch of the 1-DDT SAM with the scale bar corresponding to 10.8 adu mW⁻¹ s⁻¹. The relationship between temperature and peak intensities of the T and G bands are shown in (b), where an increase in the solution temperature causes the T band to attenuate and the G band to increase. (M.Rycenga and Zhipeng Wang et.al. 2009)

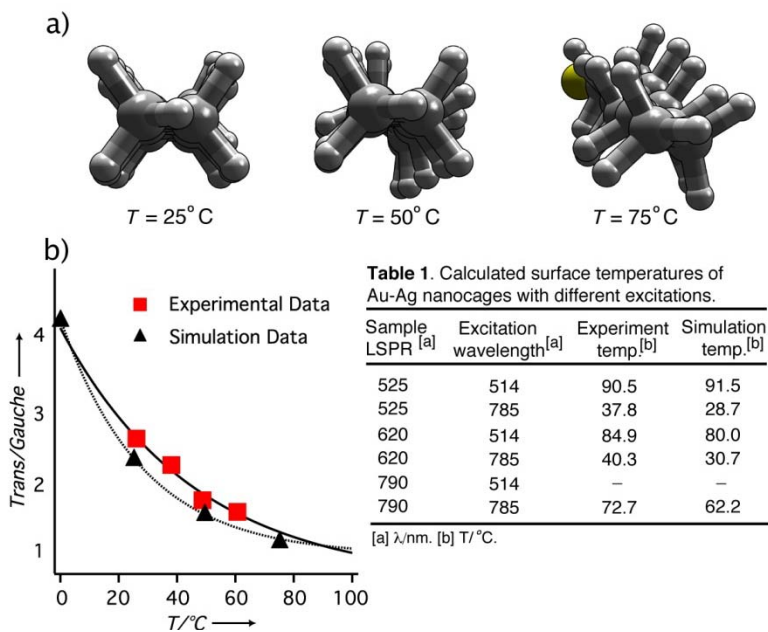


Figure A-3. Results of molecular dynamic simulations of 1-DDT SAMs (a) Optimized alkane chain conformation of a 1-DDT SAM on a Au surface at three different temperatures. The cartoons are looking down the carbon chain toward the sulfur group where grey is carbon, white is hydrogen and yellow is sulfur. When the temperature was increased, the torsion of the alkyl chains increased and there is a higher population of end-gauche and gauche conformations as evidenced by the increasing non-planar character of the alkane thiol molecule. (b) A plot of the Trans/gauche ratio of the 1-DDT SAM from experimental (square markers) and simulation (triangle markers) data. Table 1 shows the derived temperatures of the 1-DDT SAMs on the nanocages from the fits in (b). (M.Rycenga and Zhipeng Wang et.al. 2009)

(Reference: M.Rycenga and Zhipeng Wang et.al. “Probing the photothermal effect of Au-based nanocages with SERS”, *Angewante. Chemie. Int. Ed.* 2009, 48, 9924-9927)

Project B

Microbial Response to Simulated CO₂ Leakage from Geologic Sequestration Sites (advisor: Professor Young-Shin Jun and Professor Yinjie Tang)

This study mainly investigates the survival and growth of *Shewanella oneidensis* MR-1 under CO₂ stress due to CO₂ leakage from geologic sequestration (GS) sites. In control experiments, under high-pressure nitrogen gas (up to 500 psi), MR-1's physiology was apparently not affected. Under low-pressure CO₂ ($P_{\text{CO}_2} = 0.15$ psi), however, the growth of MR-1 was significantly reduced compared to the control. When the CO₂ pressure was over 15 psi, the pH in the aqueous medium could drop from 6.5 to below 5.6, at which point the growth of MR-1 in the medium came to a complete halt. Scanning electron microscopy and atomic force microscopy images revealed significant cell structure deformation and cellular content release. However, if *Shewanella* cells formed biofilms, the number of viable cells significantly improved compared to the suspended aqueous culture under $P_{\text{CO}_2} = 150$ psi. The presence of calcites in the medium alleviated CO₂ stress on growth and increased bacterial viability by pH buffering as well. Finally, a general two-parameter mathematical model was developed to describe the microbial responses under different CO₂ pressures and exposure times. The current work provides useful information for understanding the potential ecological impact of CO₂ leakage near GS sites and will help us indirectly and inexpensively identify potential leakage.

Experimental set-up (Fig B-1)

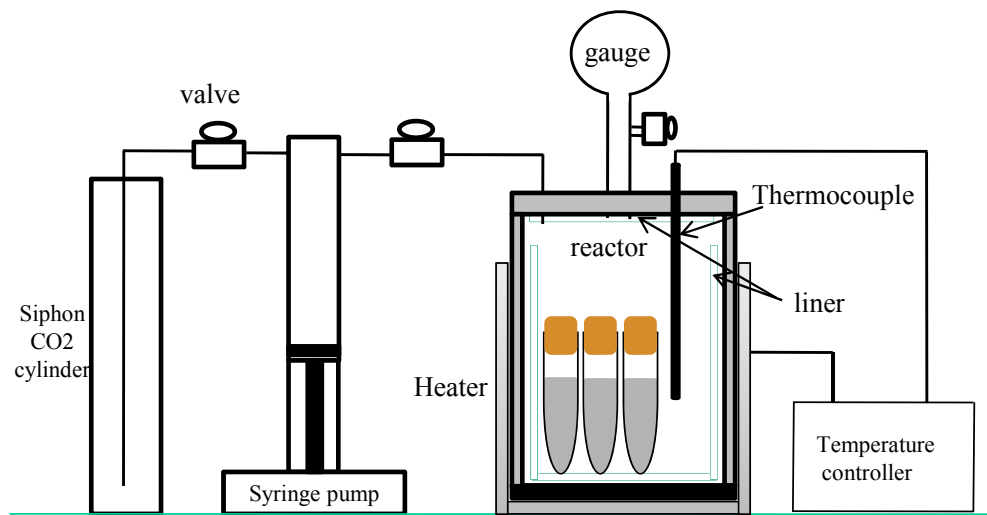
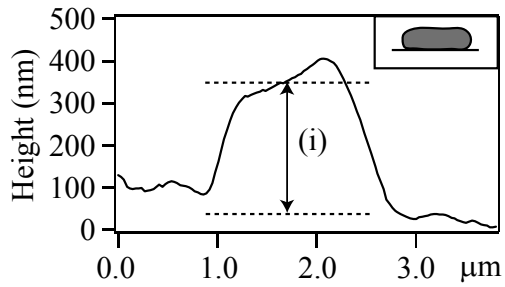
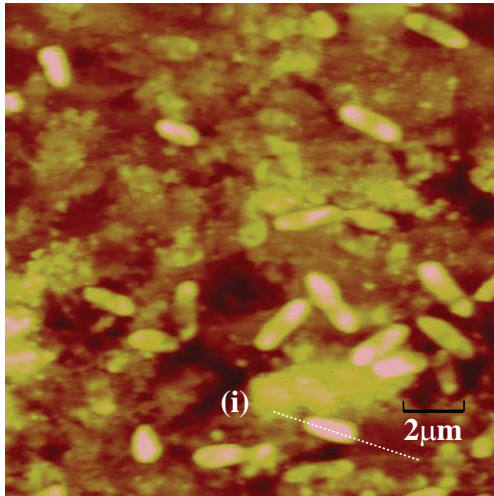


Figure B-1 Experimental set-up for CO₂ shock on *Shewanella oneidensis* MR-1 in liquid medium (Schematic Picture of the reactor)

A. Before CO₂ shock



B. After CO₂ shock for 5 min

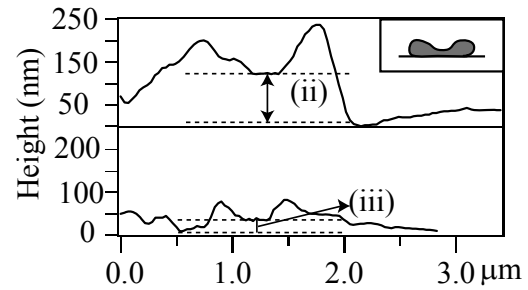
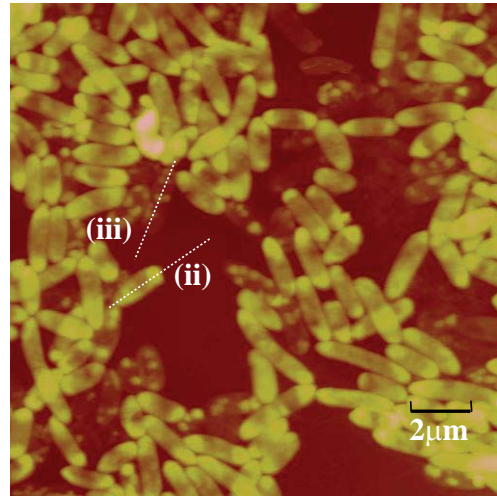


Figure B-2. The AFM (Atomic Force Microscopy) images for *Shewanella oneidensis* MR-1 before and after the CO₂ shock (5min). (Wu B et.al. submitted)

(References: Bing Wu, Hongbo Shao, Zhipeng Wang, Yandi Hu, Yinjie Tang, Young-Shin Jun, Environ. Sci. Technol. Submitted)

References

- Adams LK, Lyon DY, Alvarez PJJ 2006 Comparative eco-toxicity of nanoscale TiO₂, SiO₂, and ZnO water suspensions. *Water Research* 40(19):3527-3532
- Ao CH, Lee SC 2005 Indoor air purification by photocatalyst TiO₂ immobilized on an activated carbon filter installed in an air cleaner. *Chemical Engineering Science* 60(1):103-109
- Aruoja V, Dubourguier HC, Kasemets K, Kahru A 2009 Toxicity of nanoparticles of CuO, ZnO and TiO₂ to microalgae *Pseudokirchneriella subcapitata*. *Science of the Total Environment* 407(4):1461-1468
- Auffan M, Rose J, Wiesner MR, Bottero JY 2009 Chemical stability of metallic nanoparticles: A parameter controlling their potential cellular toxicity in vitro. *Environmental Pollution* 157(4):1127-1133
- Azeredo, J.; Lazarova, V.; Oliveira, R. 1999 Methods to extract the exopolymeric matrix from biofilms: A comparative study. *Water Sci. Technol.* 39, 211-218
- Bradford, M. and M. Rapid 1976 Sensitive Method for the Quantitation of Microgram Quantities of Protein Utilizing the Principle of Protein-dye Binding. *Analytical Biochemistry* 72, 248-25449
- Brayner R 2008 The toxicological impact of nanoparticles. *Nanotoday* 3:48-55
- Brunner, T. J.; Wick, P.; Manser, P.; Spohn, P.; Grass, R. N.; Limbach, L. K.; Bruinink, A.; Stark, W. J. 2006 In vitro cytotoxicity of oxide nanoparticles: Comparison to asbestos, silica, and the effect of particle solubility. *Environ. Sci. Technol.* 40, 4374-4381
- Chen D, David YH, Pui D 1995 Electrospraying of conducting liquids for monodisperse aerosol generation in the 4 nm to 1.8 um diameter range. *J. Aerosol Sci.* 26:963-977
- Chen KL, Elimelech M 2008 Interaction of Fullerene (C-60) Nanoparticles with Humic Acid and Alginate Coated Silica Surfaces: Measurements, Mechanisms, and Environmental Implications. *Environ Sci. Technol.* 42(20):7607-7614
- Cloupeau MP-F, B. 1989 Electrostatic spraying of liquids in cone-jet mode. *J. Electrostatics* 22:135
- Cloupeau MP-F, B. 1990 Electrostatic spraying of liquids: Main functioning modes. *J. Electrostatics* 25:165
- Cloupeau, M. 1994a Recipes for Use of EHD Spraying in Cone-jet mode and Notes on Corona Discharge Effects. *J. Aerosol. Sci.* 25, 1143-1157

Cloupeau, M.; Prunet-Foch, B. 1994b Electrohydrodynamic spraying functioning modes: A critical review. *J. Aerosol. Sci.* 25, 1021

Dubois, M.; Gilles, K. A.; Hamilton, J. K.; Rebers, P. A.; Smith, F. 1956 Colorimetric Method for Determination of Sugars and Related Substances. *Anal. Chem.* 28, 350-356

Eboigbodin, K. E.; Biggs, C. A. 2008 Characterization of the Extracellular Polymeric Substances Produced by *Escherichia coli* Using Infrared Spectroscopic, Proteomic, and Aggregation Studies. *Biomacromolecules* 9, 686-695

Edward J. Wolfrum, Jie Huang, Daniel M. Blake, Pin-Ching Maness, Zheng Huang, and Janene First. 2002 Photocatalytic Oxidation of Bacteria, bacterial and fungal spores, and model biofilm components to carbon dioxide on titanium dioxide-coated surfaces. *Environ. Sci. Technol.* 36, 3412-3416

Fan Yang, Larry G. Moss and George N. Philips, Jr. 1996 The molecular structure of green fluorescence protein. *Nature Biotechnology* 14, 1246-1251

Farré, M.; Gajda-Schranz, K.; Kantiani, L.; Barceló, D. 2009 Ecotoxicity and analysis of nanomaterials in the aquatic environment. *Analytical and Bioanalytical Chemistry.* 393, 81-95

Franklin NM, Rogers NJ, Apte SC, Batley GE, Gadd GE, Casey PS 2007 Comparative Toxicity of Nanoparticulate ZnO, Bulk ZnO, and ZnCl₂ to a Freshwater Microalga (*Pseudokirchneriella subcapitata*): The Importance of Particle Solubility. *Environ. Sci. Technol.* 41:8484-8490

Gogoi, S. K.; Gopinath, P.; Paul, A.; Ramesh, A.; Ghosh, S. S.; Chattopadhyay, A. 2006 Green fluorescent protein-expressing *Escherichia coli* as a model system for investigating the antimicrobial activities of silver nanoparticles. *Langmuir.* 22, 9322-9328

Handy RD, von der Kammer F, Lead JR, Hasselov M, Owen R, Crane M 2008 The ecotoxicology and chemistry of manufactured nanoparticles. *Ecotoxicology* 17:287-314

Horie M, Nishio K, Fujita K, Kato H, Nakamura A, Kinugasa S, Endoh S, Miyauchi A, Yamamoto K, Murayama H and others 2009 Ultrafine NiO Particles Induce Cytotoxicity in Vitro by Cellular Uptake and Subsequent Ni(II) Release. *Chemical Research in Toxicology* 22(8):1415-1426

Hu Chun, Lan YQ, Qu JH, Hu XX, Wang AM 2006 Ag/AgBr/TiO₂ Visible light photocatalyst for destruction of Azodyes and Bacteria. *J. Phys. Chem. B* 110, 4066-4072

Hu XK, Cook S, Wang P, Hwang HM 2009 In vitro evaluation of cytotoxicity of engineered metal oxide nanoparticles. *Science of the Total Environment* 407(8):3070-3072

Ji, S. L.; Ye, C. H. 2008 Synthesis, growth mechanism, and applications of zinc oxide nanomaterials. *J. Mater. Sci. Technol.* 24, 457-472

Kang S, Herzberg M, Rodrigues DF, Elimelech M 2008a Antibacterial effects of carbon nanotubes: Size does matter. *Langmuir* 24(13):6409-6413

Kang S, Mauter MS, Elimelech M 2008b Physicochemical determinants of multiwalled carbon nanotube bacterial cytotoxicity. *Environmental Science & Technology* 42(19):7528-7534

Kang S, Mauter MS, Elimelech M 2009 Microbial Cytotoxicity of Carbon-Based Nanomaterials: Implications for River Water and Wastewater Effluent. *Environ. Sci. Technol.* 43:2648-2653

Kim BH, Kim DW, Cho D, Cho SY 2003 Bactericidal effect of TiO₂ photocatalyst on selected food-borne pathogenic bacteria. *Chemosphere.* 52, 277-281

Kwak SY, Kim SH, Kim SS 2001 Hybrid organic/inorganic reverse osmosis (RO) membrane for bactericidal anti-fouling. 1. Preparation and characterization of TiO₂ nanoparticle self-assembled aromatic polyamide thin-film-composite (TFC) membrane. *Environmental Science & Technology* 35(11):2388-2394

Kwiatkowska J, Matuszewska E, Kuczynska-Wisnik D, Laskowska E 2008 Aggregation of *Escherichia coli* proteins during stationary phase depends on glucose and oxygen availability. *Research in Microbiology* 159(9-10):651-657

Limbach LK; Li, Y.C.; Grass, R.N.; Brunner, T.J.; Hintermann, M.A.; Muller, M.; Gunther, D.; Stark, W.J. 2005 Oxide nanoparticle uptake in human lung fibroblasts: Effects of particle size, agglomeration, and diffusion at low concentrations. *Environ. Sci. Technol.* 39, 9370-9376

Limbach LK, Wick P, Manser P, Grass RN, Bruinink A, Stark WJ 2007 Exposure of engineered nanoparticles to human lung epithelial cells: Influence of chemical composition and catalytic activity on oxidative stress. *Environmental Science & Technology* 41(11):4158-4163

Liu, H.; Fang, H. H. P. 2002 Extraction of extracellular polymeric substances (EPS) of sludges. *J. Biotechnol.* 95, 249-256

Mauter MS, Elimelech M 2008 Environmental applications of carbon-based nanomaterials. *Environmental Science & Technology* 42(16):5843-5859

M.Rycenga, Zhipeng Wang, Eric Gordon, Claire M. Cobley, Andrea G.Schwartz, Cynthia S.Lo and Younan Xia. 2009 Probing the Photothermal Effect of Au-based nanocages with Surface Enhanced Raman Scattering (SERS). *Angewante. Chemie. Int. Ed.* 48 (52):9924-7

Muysen, B. T. A.; De Schamphelaere, K. A. C.; Janssen, C. R. 2006 Mechanisms of chronic waterborne Zn toxicity in *Daphnia magna*. *Aquat Toxicol.* 77, 393-401

Navarro, E. P., F.; Wagner, B.; Marconi, F.; Kaegi, R.; Odzak, N.; Sigg, L.; Behra, R. 2008 Toxicity of Silver Nanoparticles to *Chlamydomonas reinhardtii*. *Environ. Sci. Technol.* 42, 8959-8964

Oberdorster G, Oberdorster E, Oberdorster J 2005 Nanotoxicology: An emerging discipline evolving from studies of ultrafine particles. *Environmental Health Perspectives* 113(7):823-839

O. Seven, B. Dindar, S. Aydemir, D. Metin, M.A. Ozinel, S.Icli 2004 Solar catalytic disinfection of a group of bacteria and fungi aqueous suspensions with TiO₂, ZnO and Sahara Desert dust. *Journal of Photochemistry and Photobiology A: Chemistry* 165, 103-107

Ozturk,S.; Aslim,B. 2008 Relationship between chromium (VI) resistance and extracellular polymeric substances (EPS) concentration by some cyanobacterial isolates. *Environ. Sci. Pollut. Res.* 15, 478-480

Palmiter, R. D. 2004 Protection against zinc toxicity by metallothionein and zinc transporter 1. *PNAS.* 101, 4918-4923

Panoff,J.-M.; Priem, B.; Morvan, H.; Joset, F. 1988 Sulphated exopolysaccharides produced by two unicellular strains of cyanobacteria, *Synechocystis* PCC 6803 and 6714. *Arch. Microbiol.* 150, 558-563

Park KW, Choi JH, Kwon BK, Lee SA, Sung YE, Ha HY, Hong SA, Kim HS and Andrzej Wieckowski 2002 Chemical and Electronic effects of Ni in Pt/Ni and Pt/Ru/Ni Alloy Nanoparticles in methanol electrooxidation. *J. Phys. Chem. B.* 106, 1869-1877

Reddy, K. J.; Haskell, J. B.; Sherman, D. M.; Sherman, L. A. 1993 Unicellular, Aerobic Nitrogen-Fixing Cyanobacteria of the Genus *Cyanothece*. *J. Bacteriol.* 175, 1284-1292

Saleh NB, Pfefferle LD, Elimelech M 2008 Aggregation Kinetics of Multiwalled Carbon Nanotubes in Aquatic Systems: Measurements and Environmental Implications. *Environ. Sci. Technol.* 42(21):7963-7969

Sarah Klosek and Daniel Raftery 2001 Visible light driven V-doped TiO₂ Photocatalyst and its photooxidation of Ethanol. *J. Phys. Chem. B* 105, 2815-2819

Schipper, O. Nanoparticle agglomeration restricts uptake into living cells. *Environ. Sci. Technol.* 2005, 39, 473

Sun Yugang and Younan Xia. 2002 Shape-Controlled Synthesis of Gold and Silver Nanoparticles. *Science*. 298, 2176-2179

Sutherland, I. W. 2001 Biofilm exopolysaccharides: a strong 337 and sticky framework. *Microbiology*. 147, 3-9

Tang YJ, Ashcroft JM, Chen D, Min GW, Kim CH, Murkhejee B, Larabell C, Keasling JD, Chen FQF 2007 Charge-associated effects of fullerene derivatives on microbial structural integrity and central metabolism. *Nano Letters* 7(3):754-760

Tang, Y. J.; Shui, W. Q.; Myers, S.; Feng, X. Y.; Bertozzi, C.; Keasling, J. D. 2009 Central metabolism in *Mycobacterium smegmatis* during the transition from O₂-rich to O₂-poor conditions as studied by isotopomer-assisted metabolite analysis. *Biotechnol. Lett.* 31, 1233-1240

Teitzel,G.M.; Parsek,M.R. 2003 Heavy Metal Resistance of Biofilm and Planktonic *Pseudomonas aeruginosa*. *Appl. Environ. Microbiol.* 69, 2313-2320

Thill,A.; Zeyons, O.; Spalla, O.; Chauvat, F.; Rose, J.; Auffan, M.; Flank, A.M. Cytotoxicity of CeO₂ nanoparticles for *Escherichia coli*. Physico-chemical insight of the cytotoxicity mechanism. *Environ. Sci. Technol.* 2006, 40, 6151-6156

Trabelsi, L.; Houda M'sakni, N.; Ben Ouada, H.; Bacha, H.; Roudesli, S. 2009 Partial Characterization of Extracellular Polysaccharides Produced by Cyanobacterium *Arthrospira platensis*. *Biotechnol. Bioprocess. Eng.* 14, 27-31

Tsien, R. Y. 1998 The green fluorescent protein. *Annu. Rev. Biochem.* 67, 509-544.

Wang, H. H.; Wick, R. L.; Xing, B. S. 2009 Toxicity of nanoparticulate and bulk ZnO, Al₂O₃ and TiO₂ to the nematode *Caenorhabditis elegans*. *Environ. Pollut.* 157, 1171-1177

Wei Chang, Wen-Yuan Lin, Zulkarnaln Zainal, Nathan E. Williams, Kai Zhu, Andrew P. Kruzic, Russell L. Smith, and Krishnan Rajeshwar. 1994 Bactericidal

Activity of TiO₂ photocatalyst in Aqueous Media: Toward a Solar-Assisted Water disinfection system. *Environmental Science & Technology*, 28, 934-938

Wolfaardt, G. M.; Lawrence, J. R.; Headley, J. V.; Robarts, R. D.; Caldwell, D. E. 1994 Microbial Exopolymers Provide a Mechanism for Bioaccumulation of Contaminants. *Microbiol. Ecol.* 27, 279-291

Wu B, Huang R, Sahu M, Feng X, Biswas P, Tang YJ 2010a Toxicity of Cu-doped TiO₂ Nanoparticles. *Science of the Total Environment* 408:1755-1758

Wu B, Wang Y, Lee Y, Horst A, Wang Z, Chen DR, Radhakrishna S, Tang YJ 2010b Comparative Eco-toxicities of Nano-ZnO particles under aquatic and Aerosol Exposure Modes. *Environ. Sci. Technol.* 44(4), 1484-1489

Wang Z, Lee Y, Wu B, Horst A, Tang YJ, Chen DR. 2010 Antimicrobial Activities of Aerosolized Transition Metal Oxide Nanoparticles. *Chemosphere*, accepted

Yu, J.C.; Ho, W.K.; Lin, J.; Yip, K.Y.; Wong, P.K. 2003 Photocatalytic activity, antibacterial effect, and photoinduced hydrophilicity of TiO₂ films coated on a stainless steel Substrate. *Environ. Sci. Technol.* 37, 2296-2301

Zhang, X. Q.; Bishop, P. L.; Kinkle, B. K. 1999 Comparison of extraction methods for quantifying extracellular polymers in biofilms. *Water Sci. Technol.* 39, 211-218

Vita

Name	Zhipeng Wang
Date of Birth:	October 28 th , 1985
Place of Birth:	Taiyuan, Shanxi, China
Undergraduate Study: (2004~2008)	Peking University, Beijing, China B.S. Chemistry
Graduate Study: (2008~present)	Washington University in St.Louis M.S. in Environmental and Chemical Engineering (May 2010) MS Thesis Advisor: Yinjie Tang
Professional Society:	American Institute of Chemical Engineers

Publications:

M.Rycenga, Zhipeng Wang, Eric Gordon, Claire M. Cobley, Andrea G.Schwartz, Cynthia S.Lo and Younan Xia. 2009 Probing the Photothermal Effect of Au-based nanocages with Surface Enhanced Raman Scattering (SERS). *Angewante. Chemie. Int. Ed.* 48 (52):9924-7

Wang Z, Yi-Shuan Lee, Angela Horst, Kang Yisheng, Bing Wu, Da-Ren Chen and Yinjie Tang, antimicrobial effect of aerosolized transition metal oxide nanoparticles, *Chemosphere*, accepted

Wu B, Wang Y, Lee Y, Horst A, Wang Z, Chen DR, Radhakrishna S, Tang YJ 2010 Comparative Eco-toxicities of Nano-ZnO particles under aquatic and Aerosol Exposure Modes. *Environ. Sci. Technol.* 44(4), 1484-1489

Bing Wu, Hongbo Shao, Zhipeng Wang, Yandi Hu, Yinjie Tang and Young-Shin Jun. 2010 Geologic CO₂ sequestration and its ecological impact, *Environ. Sci. Technol.* submitted